Journal of Physics D:
Applied Physics

TOPICAL REVIEW • **OPEN ACCESS**

Diagnostic techniques for the interaction of non-thermal atmospheric pressure plasmas and targets

To cite this article: A Sobota *et al* 2025 *J. Phys. D: Appl. Phys.* **58** 063005

OPEN ACCESS
IOP Publishing
Journal of Physics D: Applied Physics
J. Phys. D: Appl. Phys. **58** (2025) 063005 (26pp)
https://doi.org/10.1088/1361-6463/ad94fd

Topical Review

Diagnostic techniques for the interaction of non-thermal atmospheric pressure plasmas and targets

A Sobota[1,*], E Garcia-Caurel[2] and O Guaitella[3]

[1] Eindhoven University of Technology, Eindhoven, The Netherlands
[2] LPICM, CNRS, Ecole Polytechnique, Université Paris-Saclay, 91128 Palaiseau, France
[3] LPP, CNRS, Ecole Polytechnique, Sorbonne Université, Université Paris-Saclay, 91128 Palaiseau, France

E-mail: a.sobota@tue.nl

Received 9 May 2024, revised 21 August 2024
Accepted for publication 20 November 2024
Published 29 November 2024

Abstract

The interaction of non-thermal atmospheric pressure plasmas and targets of various properties is an interdisciplinary area of growing interest. The understanding of the interaction mechanisms between a cold atmospheric pressure plasma and the surface of a liquid or a solid target, as well as the modifications induced inside the target, requires *in situ* study of these phenomena. Techniques for characterizing the plasma above the target are very well developed but on their own they are not sufficient for understanding the interaction with the target because the target itself must be studied while being under direct exposure to the plasma. The topic of this review are the diagnostic techniques for the characterization of the target in a plasma-target system, performed *in situ*, while under plasma exposure, time-and space- resolved. Examples also include combining the existing gas-phase techniques with the techniques that traditionally characterize the target in absence of plasma. Many approaches stem from plasma science, but also chemistry, material science, mass transport and fluid dynamics. The possibilities and limitations of the *in situ* characterization techniques for liquid or solid targets are described, with examples of applications to atmospheric pressure non thermal plasma-target systems.

Keywords: plasma diagnostics, target diagnostics, surface diagnostics, non thermal atmospheric pressure plasma, plasma target interaction

* Author to whom any correspondence should be addressed.

1. Introduction

Non-thermal atmospheric pressure plasmas (NTAPPs) operate at atmospheric pressure with an important feature that the electrons are not in thermal equilibrium with the heavy particles. This difference in temperature can be as extreme as the electrons being at several eV, while the heavy particle temperature is below 1000 K, possibly even close to room temperature. The main reason for equilibrium in e.g. DC arcs is their long lifetime, in which electrons have enough time to exchange energy with heavy particles through collisions. In NTAPPs the thermal inequilibrium is achieved either by limiting the lifetime of the discharge or by limiting the conducting current, or both. Dielectric barrier discharges (DBDs) are a good example where both those methods are used to achieve the low temperature of the heavy particles, which is important for applications on sensitive substrates, while keeping the high electron temperature, to drive the discharge and its chemistry. The dielectric barrier prevents the conducting current from flowing, which also limits the lifetime of discharges, keeping them non-thermal. There are many geometries in which DBDs operate, from classical volume DBDs between two parallel-plate electrodes where at least one is covered by a dielectric, to surface DBDs, to plasma jets etc. Corona discharges are an example of short-lived discharges with conducting current limitation, as the discharge is never allowed to reach the counter electrode. When using RF excitation, a common method to control the temperature of heavy particles is to use modulation in the kHz range.

NTAPPs are exceptional in terms of their ability to produce extreme conditions, but on very short timescales. The electron temperatures in NTAPPs reach above 10 eV in very small volumes in space, their density reaches 10^{21} m^{-3}, the ionization fronts that move at speeds up to 10^6 m s^{-1} and the electric fields that reach above 10^6 V m^{-1}. All this makes them chemically active in the conditions far from thermodynamic equilibrium, meaning that chemical reactions are attainable that in conventional chemistry are only achievable at high gas temperatures. Even unique reaction pathways can occur because of short-lived excited states produced in NTAPPs, but not in conventional chemistry. As an example, the high density of radicals produced by these discharges at low gas temperature was responsible for the large yield of ozone produced in the first dielectric barrier discharge (DBD) patented by Siemens [1]. The limited lifetime of NTAPPs makes them suitable for interaction with sensitive materials, ensuring limited gas heating and limited current transfer to the target, while operating at atmospheric pressure.

The targets with which NTAPPs interact are more varied than for any other plasma type, because of numerous applications. The targets vary in electrical properties (excellent conductors and dielectrics but also materials in between), from solid to liquid, from relatively simple, like glass, to polymers, complex thin films and to very complex ones such as liquids used in medicine or biological tissue. Throughout this paper, 'target' is used to designate the solid material or volume of liquid exposed to the plasma as a whole and 'surface' only for the first molecular layers of the 'target', the closest to the plasma.

Because of their fast growth through space, small dimensions and short lifetime, NTAPPs feature steep gradients of almost any property in space, but also in time. That is why it is important to characterize them on an appropriate time scale. However, that is also the reason why it is important to characterize their interaction with targets *in situ*, during the interaction of plasma and the target and time-resolved. Here by *in situ* is meant 'in the relevant setup or reactor and while the plasma is in interaction with the target', which is referred to as *in operando* in other fields, especially in catalysis. We will keep *in situ* terminology throughout the article.

Plasma physics, material science, and biology use cutting-edge diagnostic tools within their respective fields. However, there is a notable shortage of techniques capable of scrutinizing the interactions occurring at the interfaces between these disciplines and at the physical interfaces between plasma and the relevant targets. Consequently, studies examining plasma-target interactions often rely on indirect methods or employ simplified experimental setups. For instance, investigations into plasma-induced polymer modifications frequently use pre- and post-treatment surface analyzes, extrapolating underlying mechanisms from variations in plasma parameters.

In recent years, there has been a growing number of attempts to implement target characterization techniques on systems involving plasma-target interaction. The implementation of these techniques faced challenges, particularly in achieving *in situ* and time-resolved measurements on surfaces or within targets directly exposed to plasma. However, the advancements in diagnostic techniques do offer insights into critical parameters such as surface charge, electric field distribution, and adsorbed chemical species during the interaction of NTAPPs and targets, crucial for a multitude of applications (biomedical applications, plasma for agriculture, indoor air treatment, CO_2 recycling and other molecules synthesis such as NH_3, nanomaterial synthesis, polymer treatments, textile functionalization, assisted combustion, etc). Figure 1 shows an overview of types of interactions of NTAPPs with targets and the available diagnostic techniques, which are discussed in this review.

The goal of this review is to provide a state-of-the-art overview of techniques that allow the characterization of the target surfaces, or of the bulk of the targets while they are under direct exposure to an NTAPP. The measurement techniques described here will be organized according to the types of parameters they allow to obtain, and the main advantages and limitations of each will be provided. Since the techniques allowing for *in situ* characterisation of the target itself differ significantly depending on whether the NTAPP is impacting a liquid or a solid, these two main types of targets will be addressed separately. The measurement techniques that allow for *in situ* analysis of the plasma itself when in contact with a target are obviously complementary and also very valuable. They are however already the subject of numerous articles, including review articles. Therefore, these techniques will only be briefly mentioned here with references to the corresponding review articles.

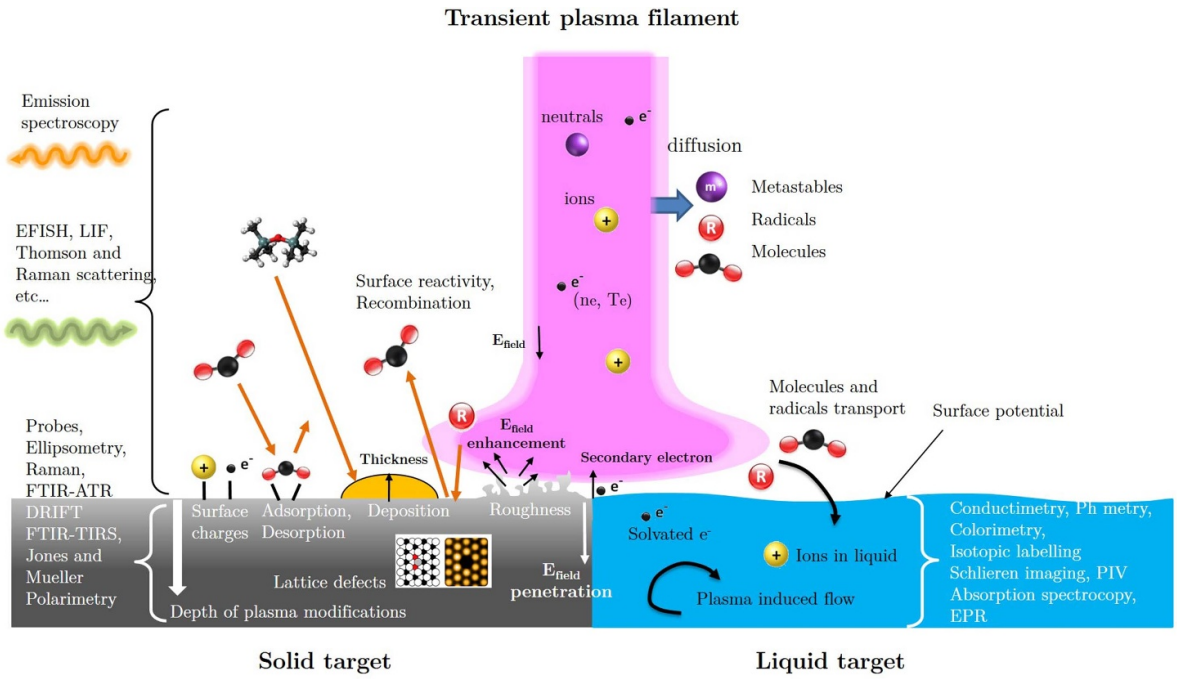

Figure 1. Interaction mechanisms between non-thermal atmospheric pressure plasma and targets and associated diagnostics. The complexity of the interaction in an NTAPP-target system as well as the diverse nature of targets often call for multiple complementary measurement techniques.

The review is therefore organized into two primary parts: sections 2 and 3 describe the diagnostics used in systems where plasmas interact with targets and section 4 brings an overview of gas-phase plasma diagnostics, but with the focus on the diagnostics done in the presence of a target. Section 4 is included because many of the diagnostic approaches that probe the plasma-target interface use (adapted) gas-phase diagnostics. Section 2 addresses the techniques relevant for the interaction of plasmas and water-based liquids. Section 3 examines the techniques used to characterize the solid targets and interfaces under plasma exposure.

2. Diagnostics of water-based liquids under plasma exposure

The interaction of NTAPPs and water-based liquids became a broadly addressed topic owing to the applications of plasma in agriculture, medicine, nanomaterial synthesis. The plasma-water system is complex in many ways. Firstly, the target (liquid) changes electrical properties over time while under plasma exposure, varying between being a poor dielectric to being a poor conductor. That causes fundamental changes in the plasma-liquid system and its electrical properties and behavior. Next, water itself is a material whose surface molecules easily re-orientate in response to the externally applied electric field, meaning that the surface conditions change greatly according to the polarity of the plasma and to whether the plasma is or is not touching the liquid surface. Furthermore, plasma-liquid interaction is not limited to the surface or a few atomic layers under the surface, instead there is a rich chemistry in the interfacial layer and bulk transport in the body of the liquid. Finally, examining the water surface while under plasma exposure is a challenging task, because of the formation of waves and Taylor cones brought on by the high electric fields supplied by NTAPPs. Changes in chemical composition at the interface or in the volume of the liquid must therefore be studied taking into account hydrodynamic phenomena. The following sub-sections first describe methods for visualizing induced fluxes in the liquid phase. The main techniques for measuring chemical composition in the liquid phase will then be described, before detailing techniques capable of investigating the gas–liquid interface in terms of chemical composition and charge. Table 1 gives an overview.

2.1. Plasma-driven liquid flow

The low ionization degree and low power dissipation, small size and short lifetime of NTAPPs suggest that their impact on the much larger liquid target bulk could be expected to be minimal, however this is not the case. This section focuses on the liquid flow induced by NTAPPs that are generated in the gas phase above the liquid.

Here a distinction has to be made between the influence of the gas flow that is at times used in the design of plasma sources (e.g. non-thermal plasma jets) and the influence of the plasma itself. It is evident that the flow of gas without the plasma present induces liquid flows when such a jet is directed at the liquid surface, however the plasma has an additional effect, which will be discussed in this section. This was qualitatively shown using schlieren imaging [12–14], imaging of the dimple dynamics [15, 16] or KI-starch liquid reagent [2, 17]. The latter is typically used to detect reactive oxygen species

Table 1. Diagnostics techniques for liquid characterization relevant for the interaction of NTAPPs and water-based liquids. Details can be found in the text.

Parameter	Technique	Comments	Reference
Liquid flow	Molecular probes, e.g. KI-starch liquid reagent	Qualitative technique, used to image transport of selected species.	[2]
	Schlieren imaging	Simpler than PIV, visualizes density gradients, challenging to do quantitative measurements.	[3]
	Particle imaging velocimetry (PIV)	Quantitative technique, well known, open source analysis scripts, literature available, expertise available in the field of transport and flow.	[4]
Density of radicals in the liquid bulk	Colorimetry	Often *ex situ*, probe molecules not entirely specific, shows saturation. Simple, ideal for visualization of the spatial distribution of molecules of interest. A large number of probe molecules available. Usable in gels and model tissue.	[5]
	Absorption spectroscopy	Done *in situ* as well as *ex situ*, quantitative.	
	Chromatography and electron paramagnetic resonance (EPR)	Done *ex situ*. EPR can provide quantitative data, proper analysis requires deep understanding of the technique and the cost is high.	
Density of solvated electrons	Absorption spectroscopy through total internal reflection	Difficult to align, depth of penetration of electrons up to 100 nm, but the only technique able to measure this property to date.	[6, 7]
Uptake of gas-phase species by the liquid	Simultaneously using a gas-phase diagnostic to measure gas-phase densities like LIF or absorption and a liquid phase diagnostic to measure the liquid phase chemistry, like absorption.	Not a direct measurement, thus detailed analysis required, takes careful alignment in the gas phase.	[8]
	Tracking of isotopes from the gas phase to the liquid phase	Direct information about the origin of e.g. O atoms that end up in the observed product; because of intricate chemistry, this is not a direct measurement of the transport for every imaginable radical, also requires detailed analysis.	e.g. [9–11]

(ROS), therefore it also clearly shows the dynamics of ROS transport in the liquid phase.

Schlieren imaging in the liquid phase is remarkably similar to the same technique used in the gas-phase diagnostics, where it can be made quantitative [3] (see also section 4.2). This technique detects gradients of refractive index in the medium through which a light beam passes. The idea is to focus the beam on a sharp spatial filter which only lets the deflected light reach the detector, thus removing the dominant signal from the light that has not been deflected [3]. The temporal resolution depends on the detector. The characteristic timescale for flow in the liquid phase is much longer than that for discharge development, so an intensified charge-coupled device (iCCD) camera is not necessary.

Interferometry is a technique that also detects gradient densities, but its temporal resolution depends on the light source rather than the detector. In [18] this technique was applied to image the development of discharges in water, however it can also be used to image shockwaves [19, 20].

Particle imaging velocimetry (PIV) [4] is at this moment the best quantitative technique available for the measurements of plasma-induced liquid flows, see example in figure 2. It involves introducing tracer particles in the liquid phase, illuminating them with a light sheet typically produced by a laser

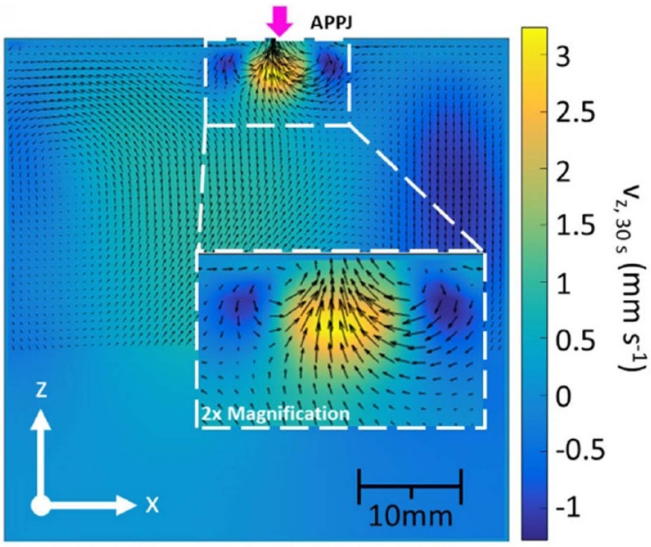

Figure 2. Typical visualization of plasma-induced liquid flow obtained by PIV. Reproduced from [21]. CC BY 4.0.

and taking images of the system in sequence using a fast framerate camera. Tracing individual particles from frame to frame allows for the determination of their speed and thus the flow field in the liquid phase. This technique is being applied in the systems where plasma is produced above the water surface [15, 21–28]. The point of attention are the physical properties of the particles. The density of the particles should be such that it matches the density of the medium in which flow is characterized. Furthermore, their size should be small enough to be able to rapidly respond to changes in flow and they should be smaller than the expected surface flow layer if surface flow is a property to be characterized. Finally, if the particles are made of polymers, it should be kept in mind that they are subject to charging if put in direct contact with the plasma.

Reflecting only on the cases where the plasma clearly impacts downwards, perpendicularly to the liquid surface, the experiments generally show a downwards liquid flow when using water-based liquids that are reasonably conductive, like saline or other ion-containing solutions, like a KI-solution [2, 17, 21, 28]. Notably, most experiments are done using plasma sources driven by positive voltage. The upwards-directed flow is measured in liquids of very low conductivity (demineralized water levels or lower) that are also not grounded or in liquids of low conductivity that contain surfactants [13, 15, 21, 28].

The direction of the flow is a consequence of force balance between electrohydrodynamic (EHD) force in the liquid due to ion movement and the force due to surface tension gradient, resulting in Marangoni flows. The surface tension gradient can be caused by temperature or chemical composition gradient at the liquid surface, where the chemical composition is severely affected by e.g. surfactants, like detergents. This is why when surfactants are present in the liquid, the plasma induces a strong surface flow because of either destruction of surfactant molecules or their displacement [23, 26]. On the other hand, liquids containing significant amounts of ions are likely to exhibit EHD-driven flows [21, 28]. Here the ion densities produced by plasma in the gas phase are not included in the consideration. They were shown to have a notable influence on the gas phase dynamics in the form of ion wind [15, 29], however the amount of ions produced by the plasma is orders of magnitude lower than the concentration and the number of ions in the liquid phase in e.g. saline solution. This is easy to calculate using ion densities in the gas phase plasma obtained through simulation, amply available in published literature. The EHD forces in the liquid are, thus, likely to be caused by the ions in the liquid, not the ions produced in the gas phase plasma.

Parameters are still missing to be able to simulate both the EHD and the Marangoni flows during the interaction of plasma and water-based liquids. For example, the current diagnostic methods for the determination of the surface tension are not compatible with the vicinity or direct contact with plasma. The research into plasma-induced liquid flows would benefit from furthering the computational efforts by using techniques from the field of transport and flows.

2.2. *Chemical changes in the bulk of the liquid*

The interaction of NTAPPs and water-based liquids gives rise to the production of chemical species in the liquid phase or transfer of species from the gas phase into the liquid phase. The species in question are numerous, with varying lifetimes and reactivities. The analysis of this system is complex—it is challenging to measure all species of interest or to determine their origin (gas or liquid phase). Reviews of plasma-liquid interactions are available [5, 30], also reviews of the chemical species expected in plasma-treated liquids [31]. This section discusses a set of diagnostics to probe the liquid phase and the transport of species across the gas–liquid interface.

Colorimetry can be used as a semi-quantitative technique. It is a classical wet-chemical analytic procedure, where indicator molecules are used to produce color forming reactions. This method can detect and visualize e.g. acidification or the abundance of a target specie [32–36]. Care should be taken as probes show saturation, thus calibration is required over the entire range of interest [37]. Visible absorption of a dosimeter specie like Fe^{3+} can also be used [38–40]. A popular technique is to use the chemiluminescence of luminol for the detection of ROSs. It is not specific to one specie, for example it will emit light when mixed with hydrogen peroxide, however in contact with plasma it emits light intensely where OH and O_2^- react with it [41]. There is a number of fluorescent probes that can be used for reactive oxygen or nitrogen species, however they are not fully specific [5]. This technique is commonly used *ex situ*, but *in situ* usage has been reported as well, especially to track the transport of species of interest through the bulk of the liquid.

The interaction of plasma and water-based liquids extends to gels (agarose, gelatine etc) and model tissue, especially for the applications in medicine. Gels can also be used in place of liquid when the deformation of the liquid surface is not

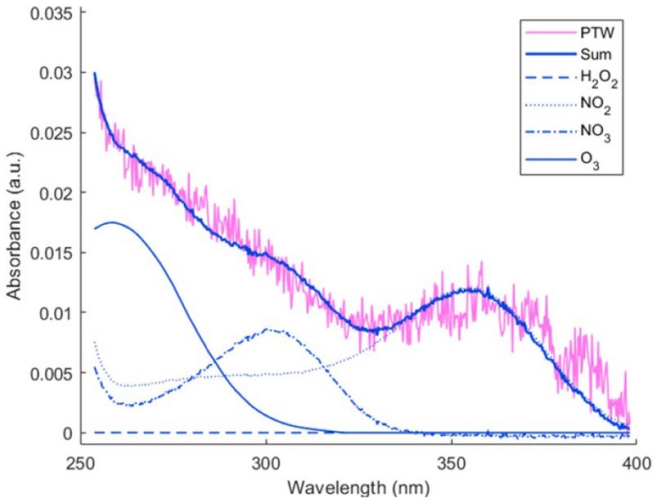

Figure 3. An example of an absorption spectrum measured on plasma-treated water (PTW) in pink, fits belonging to individual species in blue. Reproduced from [46]. CC BY 4.0.

desired. Indicator molecules or fluorescent dyes can be dispersed in the gel or tissue, after which the diagnostic procedures can be used that would otherwise be applied to a liquid target [42, 43]. This technique is typically used *ex situ*, mostly because the aim of these measurements is not to have time-resolved data, but to characterize penetration into the target over longer timescales.

Absorption spectroscopy is a technique that can be used *in situ*. In this setting, it is a derivative of absorption spectrophotometry [44] known from the 1980s [45]. Absorption spectroscopy is a very well known method used for the gas phase plasma, see section 4.2. This technique has been applied to simultaneously measure species like hydrogen peroxide, nitrate and nitrite in liquid under plasma exposure. It requires a set of absorption measurements at different wavelengths. Every absorption measurement is then described by a linear addition of different absorbing components, based on the Beer–Lambert law. The solution is found by either solving this set of linear equations, or using their *n*th derivatives in order to deconvolute the components if the solution components have overlapping absorption bands or the absorption obeys a modified Beer–Lambert law. A typical way of using this method is to perform absorption measurements in the liquid phase using a broadband light source and a spectrometer, much like they would be used in the gas phase plasma diagnostics (see section 4.2). Many species have known absorption spectra, but the difficulty is that the absorption spectra in liquids are very broad, thus easily overlapping. Typically the broad absorption features of the dominant species (e.g. nitrites, nitrates, hydrogen peroxide and ozone) hide the signature of species with low densities. Absorption spectroscopy of these species is typically done in the UV part of the spectrum, as can be seen in figure 3.

Depending on the needs of the application and the specific conditions in which the experiments are performed, it is possible to infer the density of dominant ions in the liquid phase only from the measurements of conductivity and pH of the liquid. The interest of this approach is that measuring the conductivity and pH is much easier to implement in e.g. commercial machines or systems that will be used in a setting where liquid diagnostics are not the primary concern. This approach has been demonstrated for the case where the plasma interacts with demineralized water [46], where the dominant species in the liquid phase will be nitrites, nitrates, hydrogen peroxide and ozone (short lived). The method can be adapted for use in other water-based solutions.

Further precise and sensitive techniques such as chromatography and electron paramagnetic resonance (EPR) can be used to detect radicals such as OH [47]. In order to be able to monitor short-lived species, spin traps are used. EPR can provide quantitative data. Its challenges include the fact that the results are time-averaged, it is not possible to perform this technique *in situ*, the proper analysis requires deep understanding of the technique and the cost is high. Still, this is a technique which is suitable for the detection of radicals that are poorly accessible to other techniques, for example oxygen, hydrogen, nitrogen radicals.

2.3. Processes at the plasma-liquid interface

In order to understand the chemistry induced by NTAPPs on the surface, ideally reactive species should be followed both in the plasma phase and on/in the target. It is crucial to perform the measurements *in situ*, during plasma-target interaction, due to the fact that the lifetime of most plasma-produced species is limited to the time when the plasma is present. Because of this requirement, most existing interface diagnostics are not suitable, either because they cannot be used *in situ* or because of poor time resolution. This lack of experimental techniques necessitates the use of a combination of gas-phase and liquid-phase diagnostics. A reference for the most common gas-phase diagnostics can be found in section 4. The review [48] brings a detailed list of gas-phase diagnostics used for probing plasma-liquid interactions. The analysis of results obtained by combining liquid-phase and gas-phase diagnostics requires care, however this is the most effective way to probe the plasma-liquid interface at this time. Below we will present a few ideas where the interface was probed in this manner. Although there is a number of studies that focus only on the effect of the liquid target on the gas-phase discharges, the focus in this section will be on examples that correlate the abundance of species in the gas phase to the chemical changes in the liquid.

A variety of gas-phase diagnostics can be used to probe the processes near the interface (like optical emission spectroscopy (OES), absorption, laser-based techniques, see section 4.2) and liquid-phase diagnostics the species in the liquid phase. In the diagnostics of the uptake of gas-phase species in liquids, droplets are often used [49, 50]. When using plasma, the decrease in the density of the relevant gas-phase species near the droplet train can be measured by gas-phase

diagnostics such as laser induced fluorescence (LIF) or absorption spectroscopy and the uptake by the droplets is measured in the liquid phase by using liquid-phase diagnostics. From those data, information on the interface dynamics can be obtained. In a plasma-liquid system this was done to study the OH dynamics at the interface [8]. A variation of this approach is promising for the realistic measurements of uptakes of gas-phase species not only near a liquid surface, but any surface [51].

The analysis of the chemical kinetics at the water interface can also be done using OES in the gas phase and a range of liquid-phase diagnostics [52]. Alternatively, a plasma source that has been extremely well characterized is used to treat the liquid. In combination with liquid-phase diagnostics the dynamics in the liquid close to the interface can be described [53].

For example, combining gas-phase diagnostics on the plasma and liquid-phase diagnostics, the generation and transport of atomic oxygen and hydroxyl radical was followed from the gas phase to the liquid and to the biological target cysteine in [54]. Already in 2011 [55] OH has been measured by LIF in a needle-to-plane discharge above water and the resulting dissolved OH was monitored by chemical dosimetry with terephtalic acid. The dissolved OH could, however, be produced by other processes than the solvatation of the OH detected in the gas phase. A solution was proposed to use isotopically labeled species, which are useful for tracking chemical pathways.

Isotopic labeling can be used to track the species from the gas phase to the liquid phase, also to discern between reactions happening in the plasma, its afterglow or in the liquid phase by dosing the isotopes in the appropriate phase. The use of isotopic labeling of O and H/D either in the feed gas of an NTAPP or in the water target exposed to it has allowed in [9] to identify the location where species are produced by measuring products with EPR spectroscopy. With the APPJ used in this study, the H_2O_2 detected in the target was produced in the plasma capillary while H, OH and superoxide radicals were mostly produced from interaction with the evaporating water. In [10] the COST reference jet was used to treat an aqueous solution of phenol under controlled atmosphere. The jet was fed with He/O_2 mixture with or without labeled $^{18}O_2$ and the oxidation products of the dissolved phenol were analyzed with high resolution mass spectrometry as well as gas chromatography with mass spectrometry allowing for detection of organic molecules with (labeled) oxygen. The study has shown that the oxygen atoms created in the plasma directly oxidize phenol without any pre-dissociation of H_2O. In [11] isotopic labeling was used on either oxygen in the feed gas or in the bulk water and further examined where those were included into different cysteine products. This gave insight into preferential pathways for the inclusion of the gas-phase oxygen, as well as liquid-phase derived species like the hydroxyl radicals.

Finally, Raman spectroscopy can be used to probe the evolution of chemical species near the interface. An example is [56], where the penetration depth of the excess nitrate

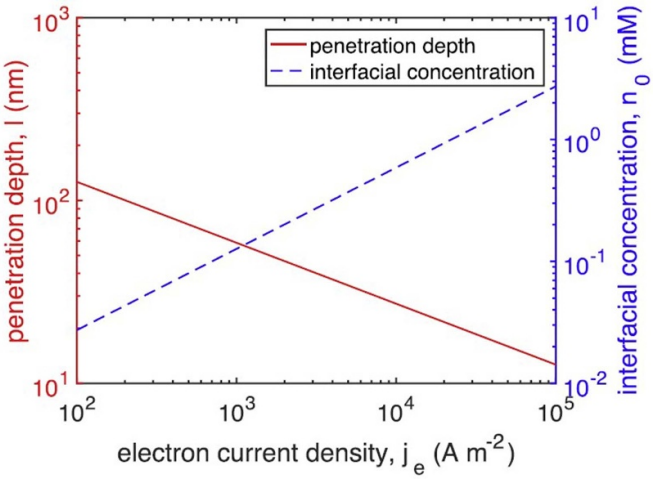

Figure 4. Penetration depth and interfacial concentration of electrons in the liquid phase, as a function of the electron current density for the case of 'neat water'. Reproduced from [59]. © IOP Publishing Ltd. All rights reserved.

concentration was measured spatially resolved in the first 100 μm of the liquid. The results show that the interfacial layer of NO_3^- has a depth of 28 μm. The shape of the meniscus may influence the interpretation of this depth.

2.3.1. Electrons. The role of electrons at the plasma-liquid interface is poorly understood, as well as their properties. The production of electrons when plasma interacts with water is thought to happen in two ways: they can be brought to the water surface by the plasma developed in the gas phase, or they can be initiated at the interface by the secondary electron emission by ion impact [57, 58], which is thought to be an important mechanism for sustaining of the plasma just above the water surface. The electrons that are produced in the gas phase are either energetic electrons that can excite, dissociate or ionize water molecules or low energy electrons that eventually become solvated. The transport of low energy electrons across the plasma-water interface is poorly understood, but pioneer research has been done on this topic [6, 7]. The diagnostic involved is the total internal reflection absorption spectroscopy, based on the Beer–Lambert law, as solvated electrons exhibit strong red absorbance around 700 nm. This technique is based on the absorption of light following the Beer–Lambert law, just like absorption in the gas phase, however the fact that the penetration depth of electrons is expected to be on a nm scale and the fact that total internal reflection is required makes this method difficult to set up. However, these are the best experimental estimates of interfacial electron densities in water under plasma exposure.

An example of results is in figure 4, showing the penetration depth and interfacial concentration of electrons in the liquid phase. Both are a function of the discharge current and the maximum penetration depth is just over 100 nm. Their role in the sustaining of the plasma above the water surface has been

studied in [60]. There, an emission mechanism was proposed where the electrons generated from ionized water molecules in the uppermost monolayers of solution are emitted into the plasma directly from the conduction band of the water. In [61] a power-law scaling was confirmed between the plasma current density and the density and the penetration depth of electrons. The penetration depth is typically below 100 nm and decreases with the plasma driving frequency.

3. Characterization of solid surfaces under plasma exposure

The purpose of using an NTAPP in direct contact with a solid is either to modify the surface properties of the solid itself (polymer or textile functionalisation, deposition, nanoparticle synthesis etc) or to take advantage of the chemical reactivity of the materials to influence the composition of the gas phase (plasma-catalysis for indoor air treatment, CO_2 conversion, NH_3 synthesis, etc). In both cases, chemical species can adsorb to the surface and structural modifications to the material can occur as well [62]. Structural changes in the target and plasma-induced surface reactivity are both strongly driven by the surface electric field strength and surface charge density that are therefore also essential to measure [63–66]. Table 2 lists the main techniques used in literature for these *in situ* analyzes under direct NTAPP exposure. The references mentioned in this table are review papers and books dedicated to the specific measurement technique but not necessarily with plasma. The examples of use of the techniques with plasma are given in the text and discussed in details there.

A large number of plasma-catalysis studies focuses on the measurements of gas compositions at the reactor outlet, as can be seen for CO_2 conversion processes with the database developed in [82]. Chemical species are sometimes measured directly in the plasma above the surface to be treated, using techniques outlined in section 4.2. However, to understand the mechanisms of plasma-surface interaction, measuring the gas composition of the effluent (even if this is done *in operando* conditions) or in the plasma phase is not enough and *in situ* analysis methods of chemical species on the surface or structural changes in the material are essential.

One of the main specificities of NTAPP compared with other surface treatment or catalysis processes is that it induces very high surface electric field (E_{surf}) and surface charge density (σ_{surf}). E_{surf} and σ_{surf} not only control the properties of the plasma itself interacting with the surface, but can also modify the physical properties of the target or alter the reactivity of adsorbed species. E_{surf} and σ_{surf} are therefore essential parameters for understanding the NTAPP-target interaction.

NTAPPs can also affect the physical properties or the target structure itself. Many of the diagnostics commonly used to characterize the structure of materials need to be operated at low pressure, ruling out the possibility of implementing them *in situ*. Nevertheless, some techniques comonly used at low pressure are now applied to NTAPPs to monitor the deposition of thin film coatings, the appearance of defects in material or the surface temperature. These include ellipsometry, Raman scattering (RS) and, in a few special cases, X ray photoelectron spectroscopy (XPS) and x-ray absorption fine structure (XAFS) which will be presented in section 3.2.

The surface analysis techniques that have been most widely used for monitoring of the surface under direct exposure to NTAPP are techniques analyzing adsorbed chemical species, and primarily different variations of infrared absorption techniques. The rest of this section details the possibilities offered by each of these techniques.

Throughout this article *in situ* denotes 'in the relevant setup or reactor and while the plasma is in interaction with the target', which often referred to as *in operando* in other fields, like catalysis. This section is limited to the techniques that are applied with the plasma present and interacting with the target.

3.1. The electric field in the target and surface charge

Surface electric field can affect adsorption and desorption processes, determining the surface reactivity in catalysis [83–85], or induce cell membrane permeation and change in intracellular electric field for biomedical applications [86, 87]. The footprint of the filamentary discharge on dielectric surface has been imaged in the past by using thermo-reactive materials or powders to freeze the path taken by filamentary discharge and obtain Lichtenberg figures [88]. These techniques have shown the difference between the shape of positive and negative streamers, as well as the increase of charge carried by a streamer as a function of the electrode gap length [89]. However the first absolute values of surface potential and pattern of adsorbed charge after filamentary discharge have been obtained with the development of electrostatic probes (or capacitive probes) for flashover studies [90–96]. The first results from the Pockels effect-based techniques came soon after [97].

This section gives an overview of the state of the art in electrostatic probes and polarimetry-based techniques. However, it should be noted that these techniques are not able to isolate and investigate separately the kinetics of charge carriers at the interface. To achieve this, there has been extensive modeling work done on the physics of electrons on the plasma-solid interface [98–101], and a theoretical framework for experimental verification has been proposed [102].

3.1.1. Electrostatic probes. Various probe geometries can be used but the principle is always to measure the voltage between a reference ground and a floating potential metal rod that is placed at a precise distance from the surface of the dielectric under study [103]. To obtain the spatial distribution of the surface potential, it is necessary to scan the surface point by point. At every point the potential measured by the probe is a convolution of the signal from the charge deposited all over the surface and relatively complex deconvolution procedure has to be applied [96]. The reduction of the noise produced by the signal treatment procedure and the miniaturization of the probe itself (down to 0.5 mm in diameter [94, 104]) have allowed to detect patterns of residual charge with typical density of few pC mm^{-2} and spatial resolution about 1 mm [96, 104]. Electrostatic probes can be used over any

Table 2. Diagnostics techniques for the characterization of the interaction of NTAPPs and solid targets.

Parameter	Technique	Comments	References
Electric field, charge density in the target	Electrostatic probes	Simple to implement, not a direct measurement, requires a model to extract the electric field and charge density values.	[67]
	Jones polarimetry using the Pockels effect	Direct measurement of the electric field in target, quantitative, target has to be an optically active crystal, requires deconvolution for the calculation of the charge density, blind to the errors in alignment, unable to account for non-ideal targets.	[68, 69]
	Mueller polarimetry using the Pockels effect	Same as above, except this technique is able to account for non-ideal targets and offers the possibility to account for errors in alignment. Much more difficult to analyze than the method above and requires 16 measurements in place of 1 per data point.	[69].
Temperature of the target	Mueller polarimetry	$\Delta T \sim 1$ K can be measured, complex analysis and 16 measurements required per data point, an optically active crystal has to be used as a target.	[70]
	Raman scattering	Spatial resolution limited by laser spot size, real surface temperature over light penetration depth, often require calibration for absolute values.	[71, 72]
	Infrared (IR) camera	Simple to implement, image of spatial distribution of surface temperature, provides the temperature of the outer surface of the reactor unless IR windows are used. Needs emissivity of studied material.	[73]
	Optical probes	Simple to implement, achievable 100 μm in diameter, less intrusive than thermocouple, indirect measurement, needs to thermalize with the target.	[74]
Adsorbed molecular species	FTIR—DRIFT	Easy sample preparation, possibility of temperature and density gradients within the sample probed, poor reproducibility of absolute intensity, only relative values, limited space for the plasma source.	[75–77]
	FTIR—ATR	Good sensitivity, mainly for thin films, small penetration depth and plasma located on the opposite side of analyzed surface.	[75–77]
	FTIR—TIRS	Beer–Lambert law directly applicable, good contact between plasma and probed target, IR-transparent pellets are needed, sample preparation can be difficult.	[75–77]
	Raman scattering	Complementary with IR absorption techniques to detect other transitions for adsorbed molecules but often less sensitive. Sensitivity can be enhanced by SERS, surface selective over light penetration depth.	[78]
Structural modification of target	Raman scattering	Detection of phonons localized at laser focal point, detection of defects in lattice. Operates in reflection, identification of peaks not always possible, fluorescence can exceed the Raman signal.	[79]
	XPS, XAS, XAFS	Probing of core electrons to analyze target atomic composition, usually possible only under high vacuum unless bright synchrotron source is used. Sample transfer under vacuum can allow analysis without surface modification in the room atmosphere.	[80]
	Ellipsometry	Depending on the target the Jones formalism can be used making it simpler than Mueller polarimetry. Especially useful for coating thickness real time measurements, easy analysis only with ideal homogeneous thin films.	[81]

type of flat dielectrics, however the time required for scanning the whole surface prevents them from being used to follow the dynamics of the charge deposition during the discharge development. In some particular geometries for which the location of the ionization wave is imposed in advance, electrostatic probes can be used to follow in time the variation of surface potential [105]. In the particular case of surface DBDs, a similar idea as the 'capacitive probe' can be used by splitting of the electrode in several segments, each of them connected to the ground through a resistor (typically a few Ohms) to measure in time the displacement current due to the surface potential in front of each segment of the electrode [106]. This technique can provide the time and space evolution of surface potential in surface DBDs. However, two main difficulties remain: (a) the splitting of the ground electrode must be done carefully to not disturb the discharge—typically the separation between the segments must be small compared to the thickness of the dielectric otherwise it has been shown that the discharge development is influenced by the electrode structure, rather than non-intrusively measured, even in the volume [107]; (b) a complex signal treatment procedure taking into account the coupling between the segments and convolution of the signal from charge over the whole surface has to be done, similarly to usual electrostatic probes [108–110].

A probe can also be used inside a target, for example in water while under plasma exposure [111]. This allows for real-time measurements during plasma-water interaction, however, the probe has to be sufficiently far away from the plasma to ensure non-intrusive measurements.

3.1.2. Pockels effect–based diagnostics of electric field and surface charge. When using electrostatic probes only the residual charge after the plasma is measured with good spatial resolution. Another type of probe used to follow the electric field dynamics in the gas phase (see section 4.3) is now commercially available, based on the Pockels effect. The sensor part is an electro-optic crystal a few millimeters in size, embedded in a protective dielectric layer, which corresponds to a total diameter of the probe of about 5 mm. These relatively large dimensions compared to the typical size of NTAPPs make it challenging to use such probes as sensors for the electric field in the plasma, however work has been done on this topic [113]. These probes can be used as a target and infer the field induced at the surface of the probe by a plasma jet impacting on it. This has been done [114] after developing a calibration procedure to relate the probe signal to the surface field by taking into account the penetration of the electric field through materials of different permittivity constituting the probe.

Imaging techniques also based on the use of electro-optic crystals have been developed in order to gain understanding on how the plasma and the target interact, how the plasma charges the surface, which electric fields it induces in the material, as well as how the plasma is modified by the target. When an electric field is applied to a crystal which lacks inversion symmetry, a change in birefringence is induced that varies linearly with the intensity of the electric field. This effect, called Pockels effect, can be used to detect the intensity of the electric

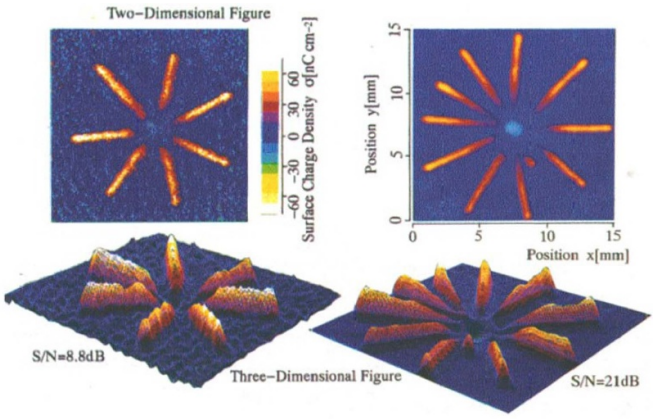

Figure 5. One of the first surface charge distribution measurements on a BSO crystal using the Pockels technique and a lock-in amplifier. Reproduced from [112]. © IOP Publishing Ltd. All rights reserved.

field induced by the plasma in the crystal by detecting a change of polarization of a light beam passing through it. This is only one of several optical effects that can be detected to characterize different physical changes induced in a target by plasma as reviewed in [115] and that will be further explained in the next section. The Pockels effect has first been used to measure surface potential in pin to plane surface discharges and compare the results with Lichtenberg figures [97]. Images of the electric field induced in the crystal can be obtained with time resolution in the ns range when using fast detection systems such as a PMT [116], streak cameras [97] or iCCD cameras [117]. One of the first surface charge distribution measurements on a BSO crystal using the Pockels technique and a lock-in amplifier is shown in figure 5. An image of surface potential pattern can be obtained in single shot which e.g. allowed to observe the transition between a randomly branching streamer regime to a stable reproducible guided streamer regime during the 2 s of the initiation of a 30 kHz coaxial atmospheric pressure plasma jet in He impacting a BSO crystal [118].

The main constraint of this technique is the need to use an electro-optic crystal (e.g. BSO [112], BGO [97], KDP [119]) as the dielectric target. These crystals have relative permittivities significantly higher than 10, which make the comparison with e.g. glass not straightforward. In order to help mimic targets that are of more interest for the applications of plasmas, the measurements can be performed with a thin layer of polymer deposited on top of the BSO as shown in [120] or material with different secondary electron emission coefficient like in [121]. Depending on the symmetry point group of the crystal used, the detected signal can be more sensitive to the electric field component perpendicular to the crystal surface or to ones parallel to the surface [117]. Finally, the crystals can be sensitive to the plasma conditions, for example become less transparent over time, turn black (this is often reversible, under the exposure to oxygen plasma), they can change shape under the influence of gas temperature in the plasma enough to disturb the polarimetric analysis.

Several points must be considered carefully when using this technique. First, the crystal should be calibrated for defects,

characteristic decay time, and linearity of the signal with intensity of the field [122, 123]. Second, the analysis of the signal obtained with only one polarization state of the light assumes that only the linear birefringence affects the detected light intensity, which can be incorrect, for example if local heating occurs in the crystal (see section 3.2.1). Third, when using this technique, the parameter which is directly deduced from the change of refractive index of the crystal exposed to a plasma is the average of the field through the thickness of the crystal. In order to get to the electric field on the surface or surface charge density, calculations are required and assumptions have to be made. A common approximation is to consider that the electric field is constant through the crystal thickness. In this case surface charge density can be calculated by considering the crystal as a planar capacitor. This approach is valid if the plasma is homogeneous over the surface on dimensions significantly larger compared to the crystal thickness, which is true for low pressure discharges [119], partial discharges in voids [124] or homogeneous DBDs [121, 122]. However, for filamentary discharges, the absolute value of the calculated surface charge density is only an estimate that depends on the characteristic size of the filaments. In [116] the surface charge appeared to depend on the thickness of the crystal used, which can be simply a consequence of a change of capacitance of the surface as modeled in [125], but also a consequence of the inaccuracy of the homogeneous field approximation through the crystal. An algorithm based on Fourier transforms and filtering has been proposed to solve this issue in [126, 127]. In [128] a different compensation procedure has been proposed to correct for the error made with the uniform field approximation, which can be used if there is a known assumption on the surface charge distribution.

This technique has been used to fully image the surface corona at atmospheric pressure and to prove that the electric field footprint is the same as the light emission obtained by (fast) imaging [112]. Later this was also confirmed in DBDs [129] and plasma jets operating in the 'bullet mode' [118, 128]. It has been used to study the formation of self-organized patterns in plane-to-plane DBDs and in He jets [130], as well as the transition from filamentary to homogeneous discharge [118, 129, 131, 132].

The results of this technique can be used for straightforward electric field measurements in an optically active target, but also to extract parameters that are typically obtainable only through modeling. For example, in a kHz He plasma jet it has been shown that the maximum amount of charge in an ionization wave reaching the target was 350 ± 40 pC and that the loss of charge during the propagation of the ionization wave in the glass capillary was approximately 7.5 pC mm^{-1} of travel distance inside the capillary [128]. The target itself could only be charged at the maximum of 22 nC mm^{-2}, irrespective of the plasma parameters [133]. Note that these data depend on the geometry of the plasma jet and the target thickness and dielectric properties. Following this, in [134] an attempt is made towards controlled charging of dielectric targets. Figure 6 shows that the surface charging can be controlled by simply tuning the operating conditions of the plasma jet.

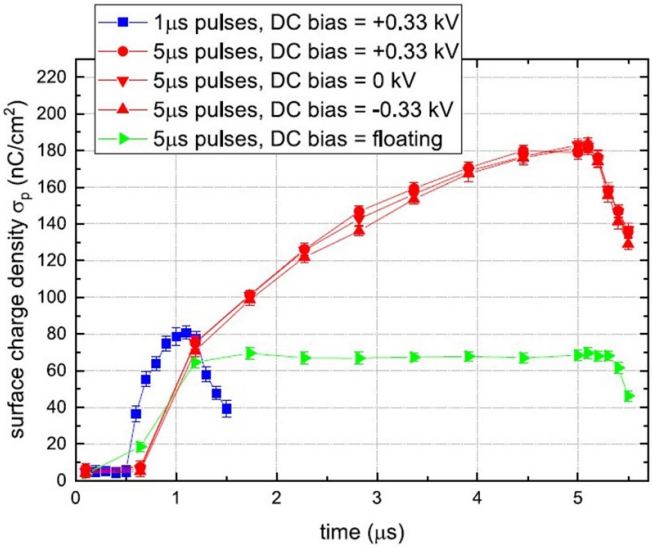

Figure 6. Surface charge density on a BSO crystal as a function of time for various cases of DC bias applied on the cryatl and pulse width applied on the plasma jet [134], using the Pockels technique. This is a measurement that directly shows the measured surface charge density on a dielectric surface and a way to control it. Reproduced from [134]. CC BY 4.0.

Similar measurements have also been performed with a jet expanding in controlled atmosphere to get insight on the species involved in charge deposition on the surface [135]. The nature of the charged species adsorbed on dielectrics remains unclear. The processes causing the release of charge from the surface and contributing to the plasma development as a secondary electron source is also unknown. It has been shown in [136, 137] that visible light is capable of photo-desorbing charge, triggering simultaneous breakdown of several plasma filaments, implying that surface charge has a low adsorption energy (<3 eV). This value corresponds to the energy of 1 eV used in modeling [138] as well as the one measured by thermo-luminescence for charge trapped in Al_2O_3 defects in DBDs [139]. Charge trapping in materials also seems to play a role on the BSO crystal used for measurements based on Pockels effect, as suggested by the slow photodecay of charge measured in [140]. In [141], based on electrical measurements, the co-existence of 'memory-charge' and 'mobile-charge' has been suggested to explain the statistical surface coverage of filaments in a planar DBD. More developments in diagnostics are therefore needed to describe in detail the dynamics of charged species on surfaces under plasma exposure.

The technique based on the Pockels effect described above only measures the electric field in the target (no other properties), while relying on a set of assumptions, for example that the setup is perfectly aligned, that there are no losses, that the target (the optically active crystal) is uniform throughout its thickness. Section 3.2.1 will present a more general way of using polarimetry in plasma-target interactions allowing to determine physical change in the target, surface temperature (T_{surf}) as well as surface field (E_{surf}) in complex targets.

3.2. Structural changes and physical parameters of targets

3.2.1. Ellipsometry and Mueller polarimetry (MP). Firstly, a quick explanation on polarimetry. When polarized light is sent onto or through a surface, a change of state of polarization can occur that can be described in terms of dichroism, birefringence and depolarization. The first two describe a change in type of polarization (e.g. linear to circular polarization) while the latter describes a change in the degree of polarization [69]. The roughness or the thickness of the material, as well as the electric field or the temperature induced inside the target are crucial parameters for the understanding of the interaction with NTAPPs and they can be obtained from techniques using polarized light.

Ellipsometry is an optical technique using the change of polarization induced by a material to retrieve physical properties of the sample via modeling analysis. Different models can be developed depending on the number of layers to be considered in the sample. Materials with homogeneous or layered bulk can be analyzed using standard ellipsometry/polarimetry, while anisotropic or depolarizing samples must be investigated using MP (see below).

Standard ellipsometry generally uses a light beam often produced by an halogen lamp reflected at an angle close to the Brewster angle. Ellipsometers are coupled to a spectrometer in order to scan the wavelengths of the radiation emitted by the source with a high spectral resolution. The reason for that is that the optical properties of the samples and the optical elements used to build ellipsometers are highly chromatic. The Brewster angle is used to increase the difference between reflected light polarized along the direction parallel and orthogonal to the plane of incidence and therefore to maximize sensitivity [142]. For successful *in situ* measurements of a surface exposed to NTAPP, the angle close to the Brewster angle can sometimes be a problem. For example, in [143], an angle of 73° is used to analyze a polystyrene surface placed 3 mm from a matrix of micro-discharges in N_2 or O_2, the width of which prevents the radiation beam used to probe the sample from passing through without moving the source between each measurement point.

Standard ellipsometry generally measures the intensity ratio (Ψ) and phase difference (Δ) between reflected light polarized parallel and perpendicular to the surface plane. The refractive index or dielectric function of the material can be directly deduced from Ψ and Δ only if the surface under study can be considered isotropic, homogeneous and infinitely thick. In all other cases it is necessary to make simplifying assumptions to establish a layer model and match experimental and calculated values of Ψ and Δ. Using these models, if for instance the material's optical constants are known, then the layer thickness can be deduced. Using the ratio of two intensities makes ellipsometry measurement fairly robust and reproducible, but since detection is performed in reflection, only perfectly flat and sufficiently reflecting samples can be easily used, making this technique especially useful for thin film characterization. The polarized light used as a probe can be sent directly onto the treated sample, allowing for real time, *in situ* measurement of the surface modification. In [144] the change of refractive index and thickness of a polymethyl methacrylate sample exposed to an Ar APPJ have been obtained from optical modeling of ellipsometry data. Similarly, polystyrene has been used in [145] as a test surface and the real time etching rate under a RF Ar jet has been studied using *in situ* ellipsometry.

MP is a more complete method for optical characterization than standard polarimetry, which allows investigating a broader diversity of samples, not just homogeneous thin films or uniform crystals. The data analysis of MP relies on the Stokes formalism instead of the Jones formalism. By measuring the change of light intensity induced by the sample for 16 different polarization states, the Mueller matrix (MM) of the sample that contains all the information of diattenuation, birefringence and depolarization can be obtained. However, a decomposition algorithm has to be applied to disentangle the information of each optical property. Different decomposition approaches exist that can be classified into three groups, product decompositions, sum decompositions and the differential or logarithmic decomposition [69, 146]. Each decomposition must be adapted to the type of sample and measurement configuration used. For instance, product decompositions assume that the MM can be written as the product of a series of matrices representing each one, a single optical property. Sum decompositions assume that the optical response 'seen' by the detector results from the incoherent superposition of a few beams coming from the sample, each one carrying a particular polarization state. Finally, the logarithmic decomposition assumes that all the polarimetric properties appear together and are homogeneously distributed in the sample. When more than one fundamental polarimetric property is present in the sample they appear entangled in the elements of the MM. The use of the logarithmic decomposition allows to disentangle the properties and to show them separately.

When the standard Pockels technique is used to analyze the electric field associated to plasma as discussed in section 3.1.2, the main optical property of interest is the linear retardance created by the electric field. If the logarithmic decomposition is applied, then the influence of the linear birefringence can be isolated from other properties such as linear diattenuation or circular retardance which can eventually be present in the sample as well. The advantage of MP over simpler optical techniques is that the MP can discriminate all the basic polarimetric properties of the sample, while with simpler techniques the results are usually interpreted in terms of one optical property (usually linear birefringence). Therefore, if a simple optical technique is used and the sample has more than one optical property appearing simultaneously, then the coupling of these optical properties may bias the interpretation of the results in terms of physical properties of the sample. Since MP is sensitive to all polarimetric properties, they can be identified to properly interpret the data in terms of sample properties. The disadvantage of MP is that it takes 16 measurements to establish a full picture of optical properties at one single setting. Thus, while the Pockels method from section 3.1.2 uses a

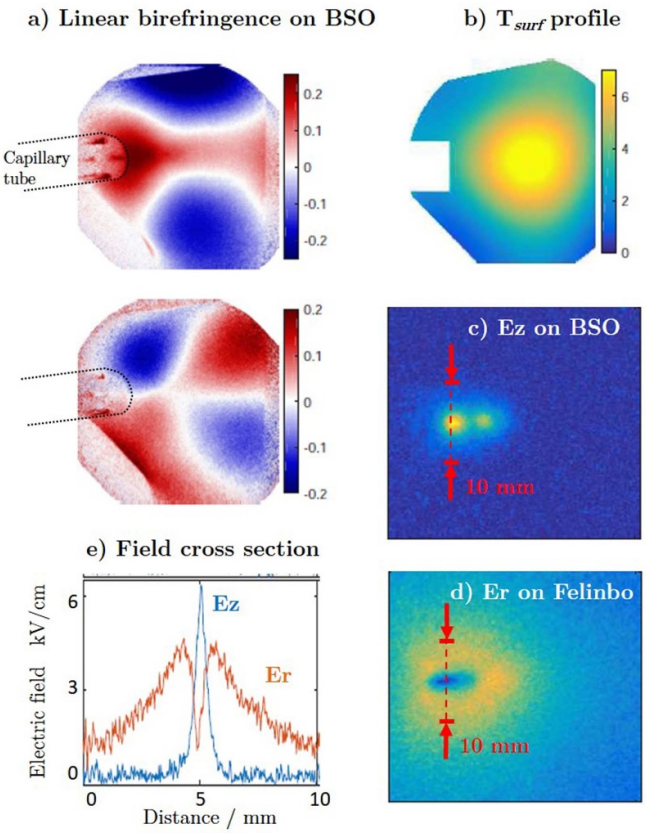

Figure 7. The only measurement of both the axial and the radial electric field in a dielectric target caused by a non-thermal atmospheric pressure plasma jet. Measurements were performed using Mueller polarimetry on electro-optic crystals ($Bi_{12}SiO_{20}$ (BSO) and Fe:$LiNbO_3$ (Felinbo)) exposed to a 30 kHz AC coaxial DBD plasma jet in Helium. (a) linear birefringence signal in the $\Gamma 0/90$ and $\Gamma 45/135$ diagonal system, (b) temperature profile (T_w) obtained simultaneously with the axial electric field, (c) electric field perpendicular to the surface of BSO (E_z), (d) radial field (E_r) obtained with Felinbo crystal in the same plasma conditions, (e) cross section comparison of the E_z and E_r field pattern at the impact point of the jet when interaction with the BSO, where the radial component is in red and the axial in blue. Adapted from [70]; [149].

minimum of two measurements to calculate the electric field, the Pockels-based MP uses 2 times 16 measurements. There are simplifications possible [147], but also overdetermination in the case of low signal/noise ratio [148].

Using MP it has been possible to identify patterns induced in electro-optic crystals under exposure to a kHz Helium jet as being a real birefringence signal induced by stress due to gradient of temperature (photo-elastic effect). As a result, both axial electric field (E_z) and wall temperature profile (T_w) inside of a $Bi_{12}SiO_{20}$ (BSO) crystal used as electro-optic probe, could be measured simultaneously as shown in figure 7 and detailed in [70, 150]. The profile shown in figure 7 corresponds to a temperature increase of less than 15 K showing the sensitivity of the technique. As already mentioned, the increase of temperature induced inside a target is important for biomedical applications or food industry, but the determination of local surface heating can also be important in the understanding of the synergy in plasma catalysis [83].

Different electro-optic crystals can also be used such as Fe:$LiNbO_3$ (Felinbo) with different symmetry point group to obtain in the same plasma condition the radial field [70]. In spite of the different materials used (BSO and Felinbo), both have high dielectric permittivity and the cross section of the field at the impact point (as in figure 7), suggesting a similar behavior of the jet impinging on both targets. Beyond the confidence gain on the field measurements because of the full optical characterization of the sample, an important advantage of MP is that similar measurements can now be performed with a coating or another material on the crystal, partly depolarizing the light.

A particularly clear example that illustrates when Pockels-based MP should be used instead of the Pockels method based on the Jones' formalism is in [151], where the electric field caused by a plasma jet was measured in a layer of cells (an organic sample) on top of a BSO crystal. In this case the approach using MP was necessary to account for the (changing) depolarization caused by the sample. This means that the sample was not perfectly transparent to the probing light, causing non-uniform losses. Not accounting for those losses by using the starndard technique from section 3.1.2 would have lead to errors in the measured electric field strength. This example also demonstrates that, thanks to the use of MP which allows to deconvolve the optical properties of the target, it is possible to study complex targets exposed to NTAPP and still succeed to deduce information on electric field, temperature or material modifications, as is the case for simpler samples when analyzed by ellipsometry or by so called 'Pockels techniques' using the Jones formalism.

3.2.2. Target temperature measured by probes, IR camera, Raman and infrared absorption. As shown in the previous section, MP can be used to trace a spatial profile of the surface temperature induced by an NTAPP in an electro-optical crystal, possibly coated with a deposit of a material of applicative interest. The surface temperature of materials exposed to NTAPP is often a key parameter in the processes developed, either because the target is temperature-sensitive (biomedical applications, polymer deposition, etc) or because temperature influences surface reactivity (plasma-catalysis, for example), and yet it is often difficult to accurately know T_{surf}. The simplest method would be to place a thermocouple on the surface being studied, as close as possible to the zone treated by the plasma. Unfortunately the presence of the thermocouple metal can modify the plasma's behavior, and the strong electric fields induced by the plasma often interfere with the proper operation of thermocouples.

Optical thermal probes made entirely of dielectric materials can be less perturbing than thermocouples. These probes generally operate on the principle of the temperature-dependent band-gap displacement of a gallium arsenide crystal placed at the end of an optical fiber, which results in a shift in the wavelength reflected by the crystal. The entire crystal must

therefore be thermalized to give the temperature of the medium in which it is immersed, but as these probes can be as small as 100 μm in diameter, thermalization can take place quite rapidly (within a few ms). These probes can measure temperature variations of a few degrees, and are sometimes used to determine the gas temperature in plasma jets [152] or in homogeneous DBD [153] but if the probe is placed in direct contact with the target, it can thermalize with it and even allow to obtain a spatial profile of temperature by scanning the surface point by point [70].

Another method often used in plasma-catalysis to measure T_{surf} is to image the material exposed to NTAPP using an infrared camera. However, the accuracy of this measurement depends on precise knowledge of the emissivity of the material under study. It is also necessary to use infrared-transparent windows, otherwise the temperature measured corresponds only to the external temperature of the reactor [154]. For this reason, in [155], an all-Sapphire reactor is used to image the spatial temperature distribution in a Ni/γ-Al_2O_3 catalyst bed exposed to a $CH_4/N_2/H_2O$ plasma.

If the infrared emission used by infrared cameras varies with the surface temperature of the material, the wavelengths absorbed in the infrared by certain materials can also vary with temperature and be used as a method of determining T_{surf}. For example, in [156] a $BaSO_4$ salt is mixed with the Ru/SiO_2 catalyst in a DBD to measure the temperature-dependent spectral shift of the S–O bond absorption band by infrared transmission (see details in section 3.3.1), giving access to an *in situ* measurement of T_{surf} with an accuracy of a few degrees, provided that the presence of $BaSiO_4$ does not modify the plasma behavior. It is the thermal deformation of crystal lattices that can affect the spectral response of vibrations in the material. The effect of temperature on the populations and energies of phonons in the target exposed to the plasma can thus also result in a spectral shift, or a variation in the relative intensity of the Stokes and anti-Stokes peaks observed in Raman [157]. The difficulty lies in finding an absolute value for T_{surf}, as the thermal deformation parameters are generally unknown, and this requires calibration by measuring the Raman signal of the material heated to a temperature imposed by a furnace. As will be detailed in the next section, other phenomena such as the appearance of defects in the material exposed to the plasma can also affect the measured Raman signal.

3.2.3. Structural modification monitored by XAFS, scanning electron microscopes (SEM) and Raman. Modifications of surface compounds are often only measured before and after plasma treatment because the techniques commonly used for surface characterization need to be performed in vacuum. Many studies dedicated to polymer treatment for isntance combine several surface diagnostics performed outside the plasma reactor (XPS, atomic force microscope, transmission electron microscope, contact angle measurement, attenuated total reflectance-Fourier-transform infrared (ATR-FTIR)) [158–163]. XPS can probe the elementary composition of the first few nm of a sample but even the so called 'ambient-pressure XPS' that are being developed work at a few mbar and cannot be used *in situ* for NTAPP [164, 165]. One step towards a quasi-*in situ* analysis of the surface is to be able to transfer the NTAPP-treated surface into the XPS instrument without passing back through the room atmosphere, which generally modifies the surface condition considerably. This is achieved by means of a sample transfer system under vacuum in [145] to study model biomolecule (peptidoglycan, bacteria membrane component) and model polymers by XPS.

By using higher-energy x-rays from a synchrotron beam, it is possible to carry out XAFS analyzes. The brilliance of today's synchrotron beams enables measurements to be carried out at high pressure, including in an atmospheric pressure packed bed DBD with a Pd catalyst in an Ar/CH4/O2 mixture [166]. The use of the XAFS technique in this study could have detected changes in the degree of oxidation of palladium under plasma exposure, but in this particular case, such changes were not observed. On the other hand, a local heating of the Pd particles much greater than the hard temperature of the catalytic bed could be demonstrated, attributed to the surface reactivity of the Pd particles.

XPS and XAFS are techniques that probe the atomic composition of the target, and as such can equally well analyze metallic or dielectric surfaces. The majority of the techniques presented in this section are mainly used on dielectric (or semiconducting for Raman) surfaces. However, we should mention a recent technique based on transient thermoreflectance measurements with a laser probe used in [167] on a gold surface, which revealed a cooling effect of the metal surface under plasma jet exposure due to charge transfer phenomena.

SEM are often used to characterize the effect of plasma treatment on a surface, but only after exposure to the plasma, as SEMs require an ultra-high vacuum chamber. Recently, however, a modification of a SEM chamber has made it possible to use a DC plasma passing through a small orifice, allowing a flow of gas to penetrate the SEM chamber as far as the surface under study, enabling analysis under direct plasma exposure of the surface [168]. The differences in surface sputtering efficiency of Cu and Ni have been studied for different gases, but adaptation to plasma sources other than DC microplasma seems difficult.

Perhaps the simplest technique for detecting structural surface changes under direct NTAPP exposure is RS. Surface RS is a vibrational spectroscopy technique that complements IR absorption techniques (see section 3.3.1), as it can detect transitions that are not active for IR absorption because they do not have any dipole moment. A practical advantage of Raman scattering is the ability to perform reflection measurements even on rough, porous surfaces. In [169], a 1 mm thick ZnO pellet on which Cu nanoparticles have been deposited is studied by RS under direct exposure to an Ar plasma jet with different mixtures of CO2, CH4 and H2. The role of vibrational excitation of H_2 and H_2O in particular in the formation of surface reaction intermediates such as acetates is highlighted by the identification of bands corresponding to the vibrations of

adsorbed C–H_3 or O–C–O bonds. Another advantage of RS is its ability to study the collective response of crystal lattices by detecting the excitation of phonons in the material. The phonon signature can then be used to highlight the creation of defects in the material exposed to the plasma, or even to estimate the surface temperature by means of the wavenumber shift of stokes and anti-stokes peaks. In [170] RS measurements were carried out on the back of a ZnO-coated steel grid directly exposed to Ar/O_2 or Ar/H_2O DBD. The appearance of a peak with a raman shift of 555 cm^{-1} is attributed to the appearance of 'surface optical phonon' corresponding to the creation of defects in ZnO linked to disorganization of the crystal lattice or grain boundaries. The reduction and the appearance of oxygen vacancies in ZnO used as catalyst support for water gas shift reaction is also studied by *in situ* RS in [62] in a DBD configuration. In [171] the impact of a pulsed repetitive nanosecond discharge is studied by RS on a thin Al_2O_3 layer deposited on a silicon wafer. The shift and distortion of the peak attributed to Si is interpreted as the result of several possible effects: the creation of phonon confinement (by destructuring the crystal lattice), heating or the creation of electron–hole pairs in the material. Raman scattering can therefore be used to gain access to certain physical modifications of the material exposed to plasma but it can also allow to study the species adsorbed on a surface by their vibrational signature. However, sensitivity to adsorbed molecules is not very high, even if better sensitivity can be achieved with nanostructured substrates (surface enhanced RS (SERS)) [157]. To study surface-adsorbed molecules, infrared absorption techniques remain the most widely used for *in situ* studies under NTAPP exposure.

3.3. Surface reactivity of adsorbed molecules

3.3.1. Infrared absorption spectroscopy. Various infrared absorption spectroscopy techniques have been developed to be applicable to a wide range of material properties. The three most widely used techniques are all based on the use of FTIR spectrometers: ATR measurements often used for thin films as in the case of polymer deposition, diffuse reflectance infrared Fourier transform spectroscopy (DRIFT) measurements and transmission infrared spectroscopy (TIRS) measurements are more often used for plasma-catalysis studies. The specular reflectance (and trans-reflectance) technique is also a possible technique but it is only applicable to perfectly smooth substrates with good reflectivity, or to thin films on a reflective substrate, which limits its applicability to very specific materials, as done in [172, 173] on Macor surface. Another interesting reflectance technique recently applied with NT-APP is the polarization modulated infrared reflection absorption spectroscopy (PM-IRRAS). The various configurations with possible coupling with a plasma source are represented on the schematics in figure 8.

All these techniques are based on the detection of infrared photon absorption by vibrational transitions characteristic of inter-atomic bonds in the material itself, or of molecules adsorbed to its surface. The differences between these techniques lie in the way infrared light interacts with the surface, depending on whether it is directly reflected (specular reflection), reflected within the material, or diffused in all directions. In most cases, especially for plasma-catalysis studies, the spectrum of the material before exposure to the gas and/or plasma flow is used as a reference, and the evolution of the transmittance (or the absorbance) obtained from the FTIR spectra then reflects the appearance or disappearance of adsorbed species.

The principle of ATR is based on the reflection of the infrared beam inside a crystal with a higher refractive index than the sample being analyzed (often a ZnSe crystal). An evanescent wave is generated at the crystal/sample interface, typically penetrating a few μm into the sample. Contact between sample and crystal must be very good, and in the absence of plasma, ATR analysis is often performed by pressing the sample onto the crystal. For ATR analysis under direct plasma exposure, this is not possible since the material being analyzed is positioned between the plasma and the crystal. The surface where the evanescent one is probing the material is therefore not the one directly in contact with the plasma. These constraints mean that *in situ* ATR with NTAPPs is only used for very thin polymer films deposited directly on the ATR crystal, or for liquid films that ensure good contact with it. This technique is often used at low pressure for studying thin film growth [174, 175] but the same can be done at atmospheric pressure. As an example, in [176] the modification of a polyethylene film deposited on a ZnSe ATR crystal is studied under exposure to a DBD of N_2/H_2. In [177] the polymerization of precursors in a liquid film is studied under direct exposure to an Ar Kinpen RF jet on a diamond ATR crystal.

The principle of DRIFT technique is to collect the light scattered in all directions by the sample's uneven surface by using a mirror shaped like an ellipsoid or a paraboloid. The DRIFT technique is widely used for plasma-catalysis studies, as it allows materials to be analyzed in powder form [178]. A major advantage of DRIFT is that no special preparation of the sample to be analyzed is required, but the downside is that quantitative interpretation of the spectra can be complex. Infrared light can either undergo multiple reflections at the particle surface (specular reflection), or actually penetrate the particle material and be diffused by it. The relative contributions of specular reflection and diffusion can explain the differences in spectra obtained by DRIFT or TIRS (see below). Various parameters of the particle bed can affect the spectra obtained by DRIFT, such as refractive index, particle size and material absorption coefficient. In particular, particles smaller than the wavelength of the infrared beam (i.e. <10 μm) are preferable to reduce the contribution of external reflection. The homogeneity and density with which the powder bed is placed in the DRIFT cell is also important, making it very difficult to achieve good reproducibility of spectral intensity from one sample to another. Consequently, only relative evolutions are truly relevant, often obtained by normalizing on a band assumed not to evolve under the conditions of the study. The Beer–Lambert law can not directly be applied for DRIFT analysis but semi-quantitative analysis can still be achieved

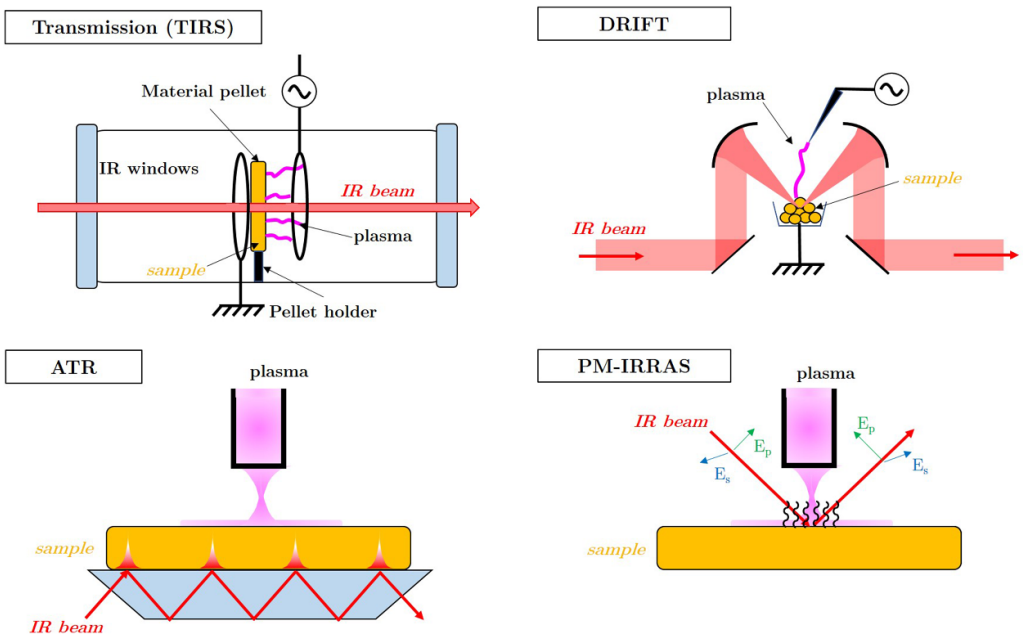

Figure 8. Main IR absorption techniques configurations used for *in situ* studies of plasma-surface interaction with NTAPPs.

applying the Kubelka-Munk approximation which suppose a semi-infinite thickness of the sample (in practice a few mm of powder bed is sufficient). Commercial DRIFT cells also offer the possibility of heating the sample under a controlled atmosphere, making it relatively easy to compare thermal catalysis processes with those of plasma-catalysis. The main difficulty for plasma-catalysis studies is to insert a plasma source in direct contact with the material in these cells, which generally have a very limited volume. For this reason, the plasma used is often a plasma jet with helium or argon as carrier gas, allowing the electrodes to be positioned at a distance from the zone of interaction between the plasma and the surface being analyzed [179–182]. It is also possible to use a pin to plane or pin to ring DBD configuration to generate streamers directly on the surface of the cup containing the material analyzed by DRIFT [183–187]. An important advantage of being able to precisely heat the sample exposed to the plasma in DRIFT cells is the ability to study adsorption mechanisms as a function of surface temperature, and in particular to perform thermal programmed desorption procedures [185].

Transmission (TIRS) is the easiest method to interpret *in-situ* (*in operando*) infrared analysis of a solid since the Beer Lambert law can be directly applied to determine transmission spectrum of the sample. However, the main difficulty in TIRS is to obtain a sample that is sufficiently transparent in the infrared to collect a signal. The sample can either be a thin film deposited on an infrared-transparent wafer, or it can be prepared by pressing powdered material in a mold to obtain a thin disk, typically around 100 μm thick (pellet). In the case of a film deposited on a wafer, the difficulty with measurements carried out directly in a plasma is to ensure that the interaction of the plasma with the supporting wafer itself does not alter the results. In the case of pellets, the mechanical strength of such a thin disk can be a problem when it comes to holding the sample in the plasma reactor and in the path of the infrared beam. For this reason, a metal grid is sometimes used as a support, but again, the presence of this grid, even at floating potential, can influence the interaction with the plasma. Finally, many materials are not sufficiently transparent for even a very thin disk to pass infrared light. This problem can be solved by diluting the material under study in an infrared-transparent powder (most often KBr), but once again, the presence of this other material can modify the mechanisms of interaction with the plasma (for example, H_2O or CO molecules adsorb on KBr surface). The small dimensions of atmospheric pressure plasmas, and the often very short characteristic diffusion lengths of the most reactive species, mean that electrode geometry must be designed very close to the material pellets used for TIRS in order to be able to study the plasma-surface interaction. This is not easy to achieve while leaving the optical path clear to allow the infrared beam to pass through the pellet. To meet these constraints, in [156, 188, 189] the KBr infrared window is used directly as a dielectric barrier in contact with a metal grid used as a ground electrode, allowing the infrared beam to pass partially through. In [190] a plane to plane DBD configuration perpendicular to the catalyst pellet is used to study toluene removal on NiO surface but this requires an inter-electrode gap of only 4 mm through which the IR beam must pass. A similar configuration is used in [62] to study the reverse water gas shift reaction on a Pd/ZnO catalyst. A pin to ring DBD configuration has also been used for volatile organic compound oxidation studies in [191]. To ensure that the plasma is in contact with the material being studied while leaving the optical path free for the infrared beam, a compromise is sometimes made by reducing the pressure in order to increase the size of the plasma discharge. In [192] for example, a ring to ring

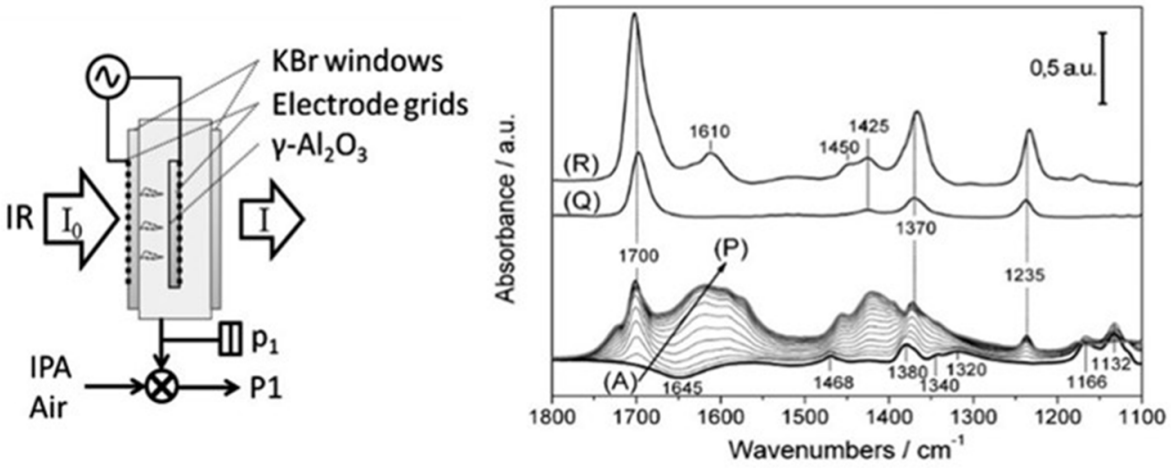

Figure 9. Experimental setup for FTIR *in situ* measurement in transmission through a γ-Al_2O_3 pellet inside a plane to plane DBD with 2 mesh electrodes and the obtained time resolved evolution of adsorbed species spectra during the oxidation of Isopropanol in air. [188] John Wiley & Sons. Copyright © 2012 WILEY-VCH Verlag GmbH & Co. KGaA, Weinheim. This is one of the pioneering works that clearly shows the temporal evolution of acetone formation on an alumina pellet with the superimposed spectra.

DBD configuration is used at 0.1 and 0.3 bar to study oxidation of primary amine functionalized SBA-15 as an example of the potential of TIRS studies. This is also the case in [193] for ammonia synthesis studied at 16 mbar or in [194] for dry reforming of methane on CeO_2 studied at 6.6 mbar for instance.

For all these techniques, whether ATR, DRIFT or TIRS, the intensity of the infrared signature of an adsorbed species is proportional to its surface density averaged over the area probed by the infrared beam. The most highly reactive species may therefore have a surface density too low to be detected because they do not accumulate enough onto the surface. The highest band intensities in the measured spectra correspond either to intermediate species whose conversion kinetics are sufficiently slow for their surface density to be detected, or to products that accumulate over time and eventually poison the surface. Figure 9 shows spectra from [188] illustrating the adsorption on γ-Al_2O_3 pellet of an initial specie of the feed gas mixture, isopropanol (IPA) in this case, followed by its conversion into acetone over relatively long time scale of 575 s. The spectra obtained for different plasma exposure time are showing the IPA initially adsorbed on the surface (absorption bands at 1468, 1380 and 1340 cm $^{-1}$) and their decay while IPA is getting converted into acetone (absorption bands at 1700, 1370 and 1235 cm $^{-1}$) by the plasma.

The absolute surface density of an adsorbed species is difficult to determine with these techniques, but when IR absorption bands reach a saturation level as a function of time, the evolution of the relative surface coverage can be analyzed, as is done for toluene oxidation byproducts on the surface of CeO_2 in [195]. The monitoring of species accumulating over the surface is very useful (for example in [190] the plasma condition in which water accumulated on the catalyst and prevented the reactions were observed) but it can be interesting to investigate on shorter time scales species that are transient on the surface. This is feasible in the case of reversible processes which lead to periodic evolution of adsorbed species by using the FTIR in the step-scan mode (the acquisition of each time step is acquired at one position of the interferogram before moving the mirror to the next interferogram point). It has been applied with μs time resolution in pulsed glow discharge at a few mbar to measure CO_2 hydrogenation in CO_2–H_2 plasma over NiUSY catalyst [196] and similar approach could be used at atmospheric pressure since time resolution in ns range can be achieved.

Other variations of infrared absorption techniques may be of interest for the study of surface-adsorbed species under exposure to NT-APPs. For instance the PM-IRRAS technique provides a highly sensitive and selective measurement of molecules adsorbed on a surface by subtracting the absorption of an IR beam polarized perpendicular or parallel to the surface on which the beam is reflected. This eliminates any contribution from the gas phase and the material, leaving only the contribution from the adsorbates. On the other hand, this technique requires surfaces with good reflectivity, limiting its applicability. In [197], the formation of carbonaceous deposits on KBr, Ni and SiO2 surfaces was monitored under exposure to a 20 kHz Ar/CH4 plasma jet.

Another vibrational spectroscopy technique that has not yet been implemented for NTAPP but that could be of great interest is the broad band sum frequency generation, which provides vibrational spectra of surface chemical groups. This method is based on the breaking of symmetry at the interface of two media, which makes the second order susceptibility different from zero [198]. This technique therefore inherently probes selectively the surface with sub-monolayer sensitivity, and it can be applied in harsh environments. For instance, it has been used to show ultrafast sub-picosecond vibrational energy transfer at the interface between air and water in [199] and it has been used to investigate growth mechanisms in atomic layer deposition system by probing surface–CH3 and–OH groups [200].

3.3.2. Isotopic exchange reactions. Isotopic labeling of molecules can be used to prove the existence of surface mechanisms in plasma molecule formation, and even to quantify their relative contribution to gas-phase processes. To discriminate between different isotopes of the same molecule, mass spectrometry is the technique most often used [201–203], but infrared absorption can also be used [204]. Due to the high cost of isotopically-labeled pure gases, this type of experiment at atmospheric pressure has sometimes to be carried out in a batch reactor (without gas flow) or with significant dilution in a noble gas. In order to obtain good detection of surface-produced molecules containing labeled atoms, these isotope exchange measurements need to be carried out over sufficiently large surfaces, which explains why the only studies to date using this technique at atmospheric pressure have all been plasma-catalyst coupling studies.

An effective approach to revealing the role of adsorbed species is to proceed in two steps: first, the surface is pre-treated with a plasma in an isotopically-labeled gas, then in a second step a plasma in an unlabeled gas produces molecules containing labeled atoms, proving the involvement of species adsorbed to the surface during the first step. For instance in [201] a pre-treatment of four different catalyst surfaces is first performed with packed bed DBD plasma in He/$^{18}O_2$. ^{18}O atoms are then being grafted during this first step on the surface catalyst. Then the oxidation of C_6H_6 in He–$^{16}O_2$ plasma is monitored downstream by mass spectrometry and the production of $C^{18}O_2$ and $C^{18}O^{16}O$ is detected even after 30 min between the pre-treatment and the C_6H_6 conversion phase proving the role of adsorbed ^{18}O on the catalyst in oxidation process under plasma exposure. A two step approach is also used in [202] with first a DBD plasma in Ar/$^{13}CO_2$) grafting carbonated species on $CeZrO_4$ supported catalyst, followed by flushing in Ar/$^{13}CO_2$ to remove weakly adsorbed species, and then a hydrogenation plasma producing CH_4. in addition a temperature program desorption procedure is performed to discriminate the different species remaining onto the surface and the various isotopically labeled molecules are measured by mass spectrometry. Similar approaches have been used to study ammonia formation in packed bed DBD monitoring either the incorporation of H atoms from the surface in ammonia produced by N_2/D_2 plasma [204], or by monitoring the proportion of ^{15}N atoms in N_2 molecules [203]. An obvious limitation of this 2-step approach is that only adsorbed species with high binding energy can remain on the surface between the pre-treatment step and the molecule conversion step, and the possible role of physisorbed species cannot be studied in this way.

4. Diagnostics in the gas phase—a reference

Gas phase diagnostics are the traditional focus in plasma research. Consequently, they are very well developed and applied in numerous variations, the community gathered around plasma physics and chemistry trusts those techniques and there is an abundance of literature including books and reviews on this topic. However, as the gas phase diagnostics are often an essential building block in the techniques developed to probe the interface between the gas phase and solid or liquid phase, this section will give a short overview of the techniques available for the gas phase diagnostics of NTAPPs. The focus is on the techniques that are or can be used when the plasma interacts with a target.

4.1. Imaging

Imaging provides information on the morphology of the discharge and its development over time. iCCD cameras are an excellent tool for this purpose, as they allow for precise gating down to sub-ns exposure times. In some cases, e.g. streamers, where the discharges are erratic in time and space, imaging is one of the main tools of characterization of the discharge. For discharges that are reproducible, next to providing data on the morphology and development over time, imaging aids the understanding of the results of other techniques. Imaging can be done with a spectral filter to track the optical emission of species of choice, or without a filter, in which case the integral spectrum corrected for the sensitivity of the camera is caught.

There has been a plethora of studies involving (iCCD) imaging of discharges either freely expanding in the gas phase or interacting with substrates. The conductivity of the target affects significantly the morphology of the discharge, as well as the intensity of the emitted light [205–211]. Dielectric targets feature typical transient DBD behavior, where discharges are short-lived and after reaching the target induce surface discharges on the target. Excellent conductors instead induce return strokes and in some cases a static diffuse discharge above the target, being sustained by the charge from the target [212].

Specifically in the interaction of plasma and water-based liquids, imaging gives clues about the nature of the interaction, as the interaction appears differently for different conductivities of the liquid and different discharge lifetimes. The interaction can be transient as in a typical DBD, it can feature a persistent discharge above the liquid surface, more common to conducting targets, or it can show both [213, 214]. In combination with OES, imaging gives information about the spatial abundance of emitting species. Research has shown that the electrical characteristics of the target have a significant influence on the spatial distribution of OH, N2, OH (through LIF) [213, 215].

Next, pattern formation has been observed in plasma-target interactions when plasma is produced in the gas phase and interacts with water-based liquids or other targets. Plasma self-organization is of importance for the development of medical devices using NTAPPs [216]. There has been a number of dedicated studies on solid targets and a thorough review is available [217]. Pattern formation is in its essence an electrostatic phenomenon, however, focusing on plasma-liquid interactions, its dynamics can, with additional data from OES, be interpreted through the importance of the nature of charge for pattern formation [218].

4.2. Population densities

Various techniques such as OES, absorption spectroscopy, (two-photon) LIF ((TA)LIF), and mass spectrometry are commonly used to determine the densities of species in NTAPPs. Review papers offer comprehensive insights into these techniques, outlining their advantages and limitations [219–226].

OES is the fastest way to get an overall picture of the radiating species found in the plasma, which is why it is typically the first type of spectroscopic information obtained on a new plasma source. Measuring the population densities in absolute numbers is, however, not straightforward. Actinometry can be used [227–229], where a trace but known amount of an inert gas, like Ar, is introduced into the gas mixture and the density of the desired species, like O, can be inferred from the ratio of intensity of emission lines of the target specie and Ar. This scheme, however, usually depends on many assumptions on the chemistry in the discharge and is thus usually accompanied by a numerical model. If desired, OES can be done from on any region of the plasma with optical access. Its temporal resolution depends on the detector, but can be at a nanosecond timescale, accommodated to follow the development of NTAPPs.

Absorption spectroscopy [222, 223] can be used to determine absolute population densities if the absorption cross section and the pathlength are known. As this is a line-of-sight technique, to obtain the density profile along the absorption path, additional measurements have to be performed, accompanied by a deconvolution technique, such as the Abel inversion for symmetrical systems or a more general Radon inversion. Depending on the desired result, either the light source or the detector can be broadband, working from the UV to the IR spectral region. The light source can be anything that emits light in the desired wavelength range, as long as its light output is stable over time. Single pass is often the norm when the detection needs to be time-resolved on the scale of the lifetime of NTAPPs, however multi-pass cells are often used in FTIR spectrometers or in cavity ring-down spectroscopy for increased sensitivity. The temporal resolution depends on the detector. It is possible to apply this technique in a plasma interacting with a target, however care has to be taken to avoid that the interaction of the probing light with the target (e.g. reflection) influences the results. Unlike OES, this technique can be used to measure ground state population densities. Like OES, this technique suffers from overlapping absorption profiles at times, thus it is necessary to verify that the absorption at the given wavelength is likely to be caused only by the target species.

(TA)LIF [223, 224] is a popular technique for the detection of species such as NO, O, OH and others in NTAPPs, owing to the fact that (i) the detection is done only in the interaction volume of the laser beam, (ii) the plasma and that the excitation-relaxation schemes are rather unique to the difference species and (iii) the detected light is at a wavelength different from the light used for excitation. A laser is used as a light source, at the wavelength resonant with a very well defined transition of the chosen species. The excited molecules or atoms then relax to another state or set of states, emitting light at wavelength(s) different from the excitation wavelength. The light is typically collected at the 90° angle with respect to the direction of the excitation laser beam. The procedure for obtaining the absolute densities of the desired species include calibration measurements and careful consideration of effects such as saturation, photo-dissociation, photo-ionization, beam shape etc. The temporal resolution of this method depends on the duration of the laser pulse, as well as the time resolution of the detector. It is rather difficult to perform very close to a target, however recently work has been done where the LIF signal was collected as close as $\approx 15\,\mu$m away from a quartz plate [51] and within $\approx 60\,\mu$m away from a liquid surface [230].

Rayleigh and Raman scattering can be used to determine the absolute densities of the scatterers [205, 231]. They are often applied to determine the amount of air entrained in noble gasses in plasma jets. The intensity of the scattered light depends on the density of the scatterers, therefore these techniques can produce a lot of signal at atmospheric pressure. Care should be taken concerning the fact that the local densities are a function of local gas temperatures. The rotational structure of the molecules obtained in Raman scattering makes it possible to determine separately the species' densities from the gas temperature. Just like with (TA)LIF, the scattering measurements are performed under the 90° angle with respect to the excitation laser beam. Temporal resolution is typically not crucial, as the goal is to measure densities that are stable in time. There are difficulties with measuring very close to the target, however when the target surface is fixed (using solid targets), the limiting factor is the laser beam width.

Quantitative schlieren imaging or laser schlieren deflectometry has also been used to determine gas mixing, in particular gas flow expansion in air. Schlieren techniques detect gradients of refractive index in the medium in which a light beam is passing by focusing the beam on a sharp spatial filter which lets only deflected light reach the detector [3]. Refractive index gradients can be induced by different factors such as gas mixture gradients (e.g. Helium in air), or temperature gradients. The deflection angle of the light in the optical system can be calibrated in order to obtain quantitative data about temperature and gas mixture [152, 232–234]. This technique is often used to also determine temperature gradients.

Mass spectrometry [225, 226] can be used for direct measurement of most species in a plasma, including ions. The technique is very powerful, for example it allows for sampling as close as possible to the grounded metallic target, it can differentiate between isotopically labeled compounds and it can measure all species in the given mass range in the same experiment. The challenge is that the technique is complex and it takes the understanding of the inner workings of the mass spectrometer to operate it properly and to be able to analyze the results. Furthermore, the plasma is always in contact with or just above a (grounded) metallic orifice, which is very valuable for probing the interaction of plasma and metals, but should be critically examined when the results are used for the understanding of the interaction of NTAPPs and other types of targets.

Finally, the electron properties such as density and temperature can be measured using several techniques. Information on the electron properties can be inferred from OES from line ratios, however that approach requires the knowledge of the chemical pathways in the plasma under examination and preferably a model. OES focusing on Stark broadening [235, 236] is a method that works on plasmas with significant electron densities, where the total line width is not dominated by other broadening mechanisms. Thomson scattering is a technique that measures the electron density as well as temperature. It is powerful in the sense that it does not depend on chemical models or on correctly determining all line broadening mechanisms. However, it takes a lot of effort to set up, one should be careful to not cause ionization or detachment in the plasma, Rayleigh scattering has to be filtered out as it is many orders of magnitude more intense than the Thomson scattering and the Raman scattering signal has to be disentangled from the total signal. The time resolution of all methods depends on the detector and the time resolution of Thomson scattering depends additionally on the length of the laser pulse. An example complication when using Thomson scattering above water is refraction and reflection of light from the water surface and the waves caused by the plasma. As the laser intensity during Thomson scattering is high, unexpected refraction or reflection can cause damage to people and equipment. Electron density was successfully measured above water surface using e.g. Stark broadening [237–242] and Thomson scattering [205, 211, 243, 244].

4.3. Electric fields

The electric field is a crucial parameter for plasma characterization. Because of the small dimensions of NTAPPs as well as their transient nature and low ionization degree, there are strict requirements for diagnostics. For example, placing any object in the vicinity will disturb the discharge. Consequently, metallic probes that are often used in low pressure plasmas cannot be used. Electric field probes fully made of dielectric materials, detecting the electric field based on the Pockels effect, are now commercially available. However, they are typically a few mm in diameter, which is bigger than the size of filamentary discharges, and they are calibrated for electric field that is uniform over dimensions larger than the probe itself. Therefore, these probes can be useful for measuring the field surrounding a setup [113, 245] or they can be used as a target themselves to deduce the field at the surface [114] but they are not used for measuring the electric field in the plasma above a target. Instead, non-intrusive optical methods can be used under certain conditions to determine the electric field and electron density in a plasma impacting on various targets. Several reviews are available on this topic [211, 246] and some of the techniques are outlined below.

Optical emission spectroscopy can be used to study plasma-surface interaction if the collected light comes from the vicinity of the surface, which is why imaging systems are often used. The methods to determine the electric field by OES from the light emitted by the plasma differ depending on the gas. The line ratio method is popular on the first negative system and second positive system of the nitrogen molecule [247–249]. Problems may arise if the peak electric field is not located at the same position as the maximum excitation rate of the two upper states of nitrogen [250]. Additionally, at atmospheric pressure those upper states are not necessarily in steady state, therefore the determination of the electric field becomes more complex, as detailed in [251, 252]. Based on this method very high spatial and temporal resolutions have been obtained in volume and surface DBDs using cross-correlation spectroscopy [247].

An OES technique based on Stark polarization spectroscopy of a forbidden and allowed He lines is available for He-containing NTAPPs [253]. The weak intensity of the forbidden line as well as its proximity to the allowed line requires sensitive detectors (an iCCD camera) and a spectrometer with sufficient resolution. At this point the measurements are limited to the head of the ionization front and electric fields above 5 kV cm^{-1} [254, 255]. kHz-driven He plasma jets interacting with targets of different types have been studied using this method [13, 212, 255, 256].

Laser-based techniques are also available for the probing of the electric field in NTAPPs. Coherent Raman scattering (CARS) measures electric field by using resonance between vibrational states of specific molecules. Four-wave mixing technique replaces the probe beam of CARS by externally applied electric field to induce a dipole in non-polar molecules [257]. This technique has been successfully used in hydrogen [258, 259], nitrogen [260] and air plasmas [261], also over water surface [262]. It allows for spatially resolved measurement of electric field with sub-nanosecond time resolution but the weak signal detected, especially from N_2, was limiting its use to relatively large plasma volume configurations. Second harmonic generation method is simpler to implement [263]. As the signal detected depends on the nonlinear susceptibility of the probed species, some uncertainties may arise when the probed gas mixture is not known. Electric field induced second harmonic generation offers to date the best temporal and spatial resolution when measuring electric fields in NTAPPs. It is a method with challenges related to the pulse energy needed to obtain usable signal, to the beam shape, to the shape of the electric field [264, 265], but it has been applied in plasmas interacting with targets [266–268].

4.4. Gas temperature

Gas temperatures are typically measured using noninvasive spectroscopic techniques, namely rotational distributions of molecules, line profiles and neutral density measurements [219, 269].

The rotational structure can be accessed by a variety of techniques, like OES, LIF or scattering. Those techniques have been briefly introduced in section 4.2. The idea is that the rotational structure of the ground state (LIF, scattering) or the excited state is obtained. It is assumed that the particles in the rotational states within one vibrational state are distributed following the Boltzmann distribution for a given rotational

temperature. By fitting the assumed distribution on the spectrum, the rotational temperature can be obtained. How well the obtained rotational temperature reflects the translational temperature, which we regard to as gas temperature, is a matter of debate. It is commonly assumed that in the general conditions of NTAPPs, the rotational temperatures will be close to equilibrium with the translational temperatures, while the vibrational temperatures are expected to be higher. This is why publications typically regard the rotational temperatures to be a good indicator of the translational gas temperatures. However, it is common that different species in the same plasma do not follow the same rotational distribution, thus the determined temperature depends on the species [270]. This technique is easily implemented, which is why it has been used extensively in systems where plasmas interact with targets.

Temperature determination from the spectral line profiles is based on the fact that some of the line broadening mechanisms depend on the gas temperature. In this case the true translational gas temperature can be determined, however depending on the conditions, the sensitivity can be lacking. For example, in NTAPPs the conditions are high pressure and high electric fields, often high electron densities. Consequently, pressure broadening is expected to be important, as well as Stark broadening, both of which will have contributions that have to be determines next to the broadening mechanisms that depend on gas temperature. Doppler broadening in this case, which could be the measure of gas temperature, will probably not be usable. Depending on the radiator, the collision partner and the transition, van der Waals or resonance broadening will be dominant [271]. For this technique to be used, it is crucial that all possible broadening mechanisms are determined.

Finally, gas temperature can be determined from the neutral density measurement, notably from Rayleigh and Raman scattering, as outlined in section 4.2.

Using temperature probes is typically not the preferred way of measuring gas temperature in NTAPPs, due to the sensitivity of these discharges to the vicinity of any foreign object, including non-metallic materials. In addition, NTAPPs feature steep gradients in both space and time, which is hard to capture with a probe whose response time is much slower than that of the plasma and whose physical dimensions are larger than the plasma. Thermocouples are not an option because they disturb the plasma and their operation is affected by the charge and high electric fields from the plasma. Still, there exist commercial probes that are dielectric and sub-mm in dimensions, that are not disturbed by the electrical characteristics of the plasma and can be inserted into the discharge with limited disturbances. If they are not made of materials that sputter under the influence of the plasma, they are the most sensitive tool for the determination of gas temperature in the plasma. They are used in plasmas interacting with targets [70, 272, 273].

5. Conclusions and outlook

A variety of diagnostics has been presented, relevant for the interaction of non-thermal atmospheric pressure plasmas and targets. A variety of targets was taken into account, from dielectrics, metallic substrates, polymers, but also water-based liquid substrates. The diagnostics are organised in four groups—diagnostics of flow in the liquid phase, electric fields in dielectrics when in contact with plasmas, diagnostics of chemical species in targets, but also probing of the chemical species at the plasma-target interface. Finally, an overview of gas-phase plasma diagnostics was given, as many of the diagnostics probing targets rely on (adapted) diagnostics previously developed for the gas phase.

Bulk target is often more accessible for diagnostics than the plasma-target interface. This is why the processes at the interface, for example in plasma-liquid systems, are often not probed directly, but the dynamics there are inferred from the measurements in the gas phase and in the bulk target. This approach requires careful analysis, but brings results. However, this also clearly outlines the needs of the community regarding new diagnostic techniques.

There is a need for fundamental data. Taking the plasma-induced liquid flow as an example, there is a need for the surface tension of water while under plasma exposure, charged species transport across the gas–liquid interface, measurements of ion densities in the plasma at the plasma-water interface, surface charge densities in general, the electric field profile in the gas phase only to make possible the proper analysis of the experimental data. In order to make it possible to also perform proper analysis and numerical modeling of the plasma-water system, there is also the need for more information on chemical reactions in the liquid phase under different conditions of conductivity, temperature, electric field etc. Plasma-catalyst coupling is another example where the fundamental data is available for classical systems without plasma, but the data relevant for the conditions when the plasma is present are just being collected. Those conditions are high electric fields, high charge density etc.

Finally, coupling experiment and the results of computational modeling has a great potential to bring insight that is not accessible otherwise.

In conclusion, the interaction of non-thermal atmospheric pressure plasmas and targets is a field that offers plenty of opportunities for the development of new diagnostic techniques for probing chemical and physical processes that are currently inaccessible. It is expected that the resulting discoveries will enable large steps in understanding the systems under research, as well as further the associated applications.

Data availability statement

This is a review article, there is no new data.

ORCID iDs

A Sobota https://orcid.org/0000-0003-1036-4513
O Guaitella https://orcid.org/0000-0002-6509-6934

References

[1] Siemens W 1857 *Ann. Phys., Lpz.* **178** 66–122
[2] Kawasaki T, Kusumegi S, Kudo A, Sakanoshita T, Tsurumaru T and Sato A 2016 *IEEE Trans. Plasma Sci.* **44** 3223–9
[3] Settles G S 2001 *Schlieren and Shadowgraph Techniques* (Springer) (available at: http://link.springer.com/10.1007/978-3-642-56640-0)
[4] Adrian R J and Westerweel J 2011 *Particle Image Velocimetry* (Cambridge University Press)
[5] Bruggeman P J *et al* 2016 *Plasma Sources Sci. Technol.* **25** 053002
[6] Rumbach P, Bartels D M, Sankaran R M and Go D B 2015 *J. Phys. D: Appl. Phys.* **48** 424001
[7] Rumbach P, Bartels D M, Sankaran R M and Go D B 2015 *Nat. Commun.* **6** 7248
[8] Oinuma G, Nayak G, Du Y and Bruggeman P J 2020 *Plasma Sources Sci. Technol.* **29** 095002
[9] Gorbanev Y, O'Connell D and Chechik V 2016 *Chem. Eur. J.* **22** 3496–505
[10] Benedikt J, Mokhtar Hefny M, Shaw A, Buckley B R, Iza F, Schäkermann S and Bandow J E 2018 *Phys. Chem. Chem. Phys.* **20** 12037–42
[11] Wende K, Bruno G, Lalk M, Weltmann K-D, von Woedtke T, Bekeschus S and Lackmann J-W 2020 *RSC Adv.* **10** 11598–607
[12] Tochikubo F, Aoki T, Shirai N and Uchida S 2017 *Jpn. J. Appl. Phys.* **56** 046201
[13] Kovačević V V, Sretenović G B, Slikboer E, Guaitella O, Sobota A and Kuraica M M 2018 *J. Phys. D: Appl. Phys.* **51** 065202
[14] Stancampiano A, Bocanegra P E, Dozias S, Pouvesle J-M and Robert E 2021 *Plasma Sources Sci. Technol.* **30** 015002
[15] Park S, Choe W, Lee H, Park J Y, Kim J, Moon S Y and Cvelbar U 2021 *Nature* **592** 49–53
[16] Guo Y, Guo X, Xu S and Shi J 2024 *J. Phys. D: Appl. Phys.* **27** 245206
[17] Mitsugi F, Kusumegi S, Nishida K and Kawasaki T 2020 *IEEE Trans. Plasma Sci.* **49** 1–6
[18] Šimek M, Hoffer P, Tungli J, Prukner V, Schmidt J, Bílek P and Bonaventura Z 2020 *Plasma Sources Sci. Technol.* **29** 064001
[19] Hoffer P, Prukner V, Schmidt J and Šimek M 2020 *Jpn. J. Appl. Phys.* **59** SHHA08
[20] Hoffer P, Prukner V, Schmidt J and Šimek M 2021 *J. Phys. D: Appl. Phys.* **54** 285202
[21] Ryan C T, Darhuber A A, Kunnen R P J, Gelderblom H and Sobota A 2024 *Sci. Rep.* **14** 17152
[22] van Rens J F M, Schoof J T, Ummelen F C, van Vugt D C, Bruggeman P J and van Veldhuizen E M 2014 *IEEE Trans. Plasma Sci.* **42** 2622–3
[23] Thagard S M, Stratton G R, Vasilev M, Conlon P and Bohl D 2018 *Plasma Chem. Plasma Process.* **38** 719–41
[24] Brubaker T R, Ishikawa K, Kondo H, Tsutsumi T, Hashizume H, Tanaka H, Knecht S D, Bilén S G and Hori M 2019 *J. Phys. D: Appl. Phys.* **52** 075203
[25] Kawasaki T, Nishida K, Uchida G, Mitsugi F, Takenaka K, Koga K, Setsuhara Y and Shiratani M 2020 *Jpn. J. Appl. Phys.* **59** SHHF02
[26] Kawasaki T, Kamasaki M, Takeuchi N and Mitsugi F 2021 *J. Appl. Phys.* **130** 243303
[27] Yang Z, Kovach Y and Foster J 2021 *J. Appl. Phys.* **129** 163303
[28] Dickenson A, Walsh J L and Hasan M I 2021 *J. Appl. Phys.* **129** 213301
[29] Sretenović G B, Iskrenović P S, Kovačević V V and Kuraica M M 2021 *Appl. Phys. Lett.* **118** 124102
[30] Zhou R, Zhou R, Wang P, Xian Y, Mai-Prochnow A, Lu X, Cullen P J, Ostrikov K K and Bazaka K 2020 *J. Phys. D: Appl. Phys.* **53** 303001
[31] Tampieri F, Gorbanev Y and Sardella E 2023 *Plasma Process. Polym.* **20** 1–7
[32] Eisenberg G 1943 *Ind. Eng. Chem., Anal. Ed.* **15** 327–8
[33] Fox J B 1979 *Anal. Chem.* **51** 1493–502
[34] Bader H and Hoigné J 1981 *Water Res.* **15** 449–56
[35] Oehmigen K, Hoder T, Wilke C, Brandenburg R, Hahnel M, Weltmann K-D and von Woedtke T 2011 *IEEE Trans. Plasma Sci.* **39** 2646–7
[36] Tarabová B, Lukeš P, Janda M, Hensel K, Šikurová L and Machala Z 2018 *Plasma Process. Polym.* **15** 1800030
[37] Tang Q, Zhang M, Wu B, Wang X, Tu X, Ostrikov K K, Liu L and Chen Q 2024 *Plasma Process. Polym.* **21** 2300229
[38] Franclemont J and Thagard S M 2014 *Plasma Chem. Plasma Process.* **34** 705–19
[39] Adhikari E R, Samara V and Ptasinska S 2018 *Biol. Chem.* **400** 93–100
[40] Kim Y H, Hong Y J, Baik K Y, Kwon G C, Choi J J, Cho G S, Uhm H S, Kim D Y and Choi E H 2014 *Plasma Chem. Plasma Process.* **34** 457–72
[41] Shirai N, Matsuda Y and Sasaki K 2018 *Appl. Phys. Express* **11** 026201
[42] Dobrynin D, Fridman G, Friedman G and Fridman A A 2012 *Plasma Med.* **2** 71–83
[43] Szili E J, Bradley J W and Short R D 2014 *J. Phys. D: Appl. Phys.* **47** 152002
[44] He B *et al* 2017 *J. Phys. D: Appl. Phys.* **50** 445207
[45] Kitamura K and Majima R 1983 *Anal. Chem.* **55** 54–56
[46] Petković J, van de Wege R, Wubs J R, van Rooij O J A P, van Oorschot J J, Huiskamp T and Sobota A 2024 *J. Phys. D: Appl. Phys.* **57** 235202
[47] Tresp H, Hammer M U, Winter J, Weltmann K-D and Reuter S 2013 *J. Phys. D: Appl. Phys.* **46** 435401
[48] Kovačević V V, Sretenović G B, Obradović B M and Kuraica M M 2022 *J. Phys. D: Appl. Phys.* **55** 473002
[49] Davidovits P, Kolb C E, Williams L R, Jayne J T and Worsnop D R 2006 *Chem. Rev.* **106** 1323–54
[50] Kolb C E *et al* 2010 *Atmos. Chem. Phys.* **10** 10561–605
[51] Wang J and Bruggeman P J 2023 *Plasma Sources Sci. Technol.* **32** 085016
[52] Kovačević V V, Dojčinović B P, Jović M, Roglić G M, Obradović B M and Kuraica M M 2017 *J. Phys. D: Appl. Phys.* **50** 155205
[53] Schüttler S, Schöne A L, Jeß E, Gibson A R and Golda J 2024 *Phys. Chem. Chem. Phys.* **26** 8255–72
[54] Stapelmann K, Myers B, Quesada M H, Lenker E and Ranieri P J 2021 *J. Phys. D: Appl. Phys.* **54** 434003
[55] Kanazawa S, Kawano H, Watanabe S, Furuki T, Akamine S, Ichiki R, Ohkubo T, Kocik M and Mizeraczyk J 2011 *Plasma Sources Sci. Technol.* **20** 034010
[56] Pai D Z 2021 *J. Phys. D: Appl. Phys.* **54** 355201
[57] Cserfalvi T and Mezei P 1996 *Anal. Bioanal. Chem.* **355** 813–9
[58] Mezei P and Cserfalvi T 2007 *Appl. Spectrosc. Rev.* **42** 573–604
[59] Rumbach P, Bartels D M and Go D B 2018 *Plasma Sources Sci. Technol.* **27** 115013
[60] Delgado H E, Elg D T, Bartels D M, Rumbach P and Go D B 2020 *Langmuir* **36** 1156–64
[61] Martin D C, Bartels D M, Rumbach P and Go D B 2021 *Plasma Sources Sci. Technol.* **30** 03LT01
[62] Sun Y, Li J, Chen P, Wang B, Wu J, Fu M, Chen L and Ye D 2020 *Appl. Catal.* A **591** 117407
[63] Bartis E A J, Luan P, Knoll A J, Hart C, Seog J and Oehrlein G S 2015 *Biointerphases* **10** 029512
[64] Neyts E C and Bal K M 2017 *Plasma Process. Polym.* **14** 1600158

[65] Vanraes P and Bogaerts A 2021 *J. Appl. Phys.* **129** 220901
[66] Bogaerts A, Neyts E C, Guaitella O and Murphy A B 2022 *Plasma Sources Sci. Technol.* **31** 053002
[67] Chen B, Lu T, Wang D and Wang Y 2018 The effect of an electrostatic probe on measurement of the surface charge *2018 IEEE Int. Conf. on High Voltage Engineering and Application (ICHVE)* vol 2 (IEEE) pp 1–4 (available at: https://ieeexplore.ieee.org/document/8642244/)
[68] Zhang B, Xue J, Chen X, Chen S, Mu H, Xu Y and Zhang G 2021 *High Voltage* **6** 608–24
[69] Garcia-Caurel E, De Martino A, Gaston J-P and Yan L 2013 *Appl. Spectrosc.* **67** 1–21
[70] Slikboer E, Sobota A, Guaitella O and Garcia-Caurel E 2018 *J. Phys. D: Appl. Phys.* **51** 025204
[71] Lundt N *et al* 2013 *Rev. Sci. Instrum.* **84** 104906
[72] Očenášek J and Voldřich J 2015 *J. Appl. Phys.* **118** 233104
[73] DeWitt D P and Nutter G D (eds) 1988 *Theory and Practice of Radiation Thermometry* (Wiley) (available at: https://onlinelibrary.wiley.com/doi/book/10.1002/9780470172575)
[74] Mikolajek M, Martinek R, Koziorek J, Hejduk S, Vitasek J, Vanderka A, Poboril R, Vasinek V and Hercik R 2020 *J. Sens.* **2020** 1–25
[75] Zaera F 2014 *Chem. Soc. Rev.* **43** 7624–63
[76] Savara A and Weitz E 2014 *Annu. Rev. Phys. Chem.* **65** 249–73
[77] Grundmeier G, von Keudell A and de los Arcos T 2015 *Plasma Process. Polym.* **12** 926–40
[78] Campion A 1990 Raman spectroscopy of molecules adsorbed on solid surfaces *Laser Applications to Chemical Analysis* vol 36 (Optica Publishing Group) p MA1 (available at: https://opg.optica.org/abstract.cfm?URI=LACA-1990-MA1)
[79] Kudelski A 2009 *Surf. Sci.* **603** 1328–34
[80] Salmeron M and Schlogl R 2008 *Surf. Sci. Rep.* **63** 169–99
[81] Auciello O and Flamm D L (eds) 1989 *Plasma Diagnostics: Surface Analysis and Interactions* (Elsevier Inc.) (available at: www.sciencedirect.com/book/9780120676361/plasma-diagnostics)
[82] Salden A *et al* 2023 *J. Energy Chem.* **86** 318–42
[83] Neyts E C 2016 *Plasma Chem. Plasma Process.* **36** 185–212
[84] Neyts E C, Ostrikov K K, Sunkara M K and Bogaerts A 2015 *Chem. Rev.* **115** 13408–46
[85] Bal K M, Huygh S, Bogaerts A and Neyts E C 2018 *Plasma Sources Sci. Technol.* **27** 024001
[86] Neyts E C, Yusupov M, Verlackt C C and Bogaerts A 2014 *J. Phys. D: Appl. Phys.* **47** 293001
[87] Babaeva N Y, Tian W and Kushner M J 2014 *J. Phys. D: Appl. Phys.* **47** 235201
[88] Thomas A M 1951 *Br. J. Appl. Phys.* **2** 98–109
[89] Bertein H 1973 *J. Phys. D: Appl. Phys.* **6** 311
[90] Davies D K 1967 *J. Sci. Instrum.* **44** 521–4
[91] Kindel E and Arndt R 1980 *Beitr. Plasmaphys.* **20** 425–34
[92] Kindel E and Arndt R 1980 *Beitr. Plasmaphys.* **20** 119–28
[93] Abdel-Salam M, Weiss P and Lieske B 1992 *IEEE Trans. Electr. Insul.* **27** 309–19
[94] Allen N and Ghaffar A 1995 Propagation of positive streamers over insulating surfaces in air *Proc. 1995 Conf. on Electrical Insulation and Dielectric Phenomena* (IEEE) pp 447–50 (available at: http://ieeexplore.ieee.org/document/483759/)
[95] Chalmers I, Lei J, Yang B and Siew W 1995 *IEEE Trans. Dielectr. Electr. Insul.* **2** 225–30
[96] Elizondo J, Krogh M, Smith D, Stoltz D, Wright S, Sampayan S, Caporaso G, Vitello P and Tishchenko N 1997 Vacuum surface flashover and high pressure gas streamers *Digest of Technical Papers. 11th IEEE Int. Pulsed Power Conf. (Cat. No.97CH36127)* vol 2 (IEEE) pp 1027–32 (available at: http://ieeexplore.ieee.org/document/674531/)
[97] Kumada A, Chiba M and Hidaka K 1998 *J. Appl. Phys.* **84** 3059
[98] Bronold F X and Fehske H 2015 *Phys. Rev. Lett.* **115** 225001
[99] Bronold F X and Fehske H 2017 *Plasma Phys. Control. Fusion* **59** 014011
[100] Thiessen E, Bronold F X and Fehske H 2019 *Plasma Sources Sci. Technol.* **28** 095024
[101] Bronold F X, Rasek K and Fehske H 2020 *J. Appl. Phys.* **128** 180908
[102] Rasek K, Bronold F X, Bauer M and Fehske H 2018 *Europhys. Lett.* **124** 25001
[103] Deng J, Matsuoka S, Kumada A and Hidaka K 2010 *J. Phys. D: Appl. Phys.* **43** 495203
[104] Kumada A, Okabe S and Hidaka K 2009 *J. Phys. D: Appl. Phys.* **42** 095209
[105] Petrishchev V, Leonov S and Adamovich I V 2014 *Plasma Sources Sci. Technol.* **23** 065022
[106] Fouracre R A, Santos E, Timoshkin I, Given M J and Macgregor S J 2006 Surface discharge propagation: the influence of surface charge *Conf. Record of the 2006 27th Int. Power Modulator Symp.* (IEEE) pp 39–42 (available at: http://ieeexplore.ieee.org/document/4216130/)
[107] van der Schans M, Sobota A and Kroesen G M W 2016 *J. Phys. D: Appl. Phys.* **49** 195204
[108] Enloe C L, Font G I, McLaughlin T E and Orlov D M 2008 *AIAA J.* **46** 2730–40
[109] Leonov S B, Petrishchev V and Adamovich I V 2014 *J. Phys. D: Appl. Phys.* **47** 465201
[110] Soloviev V R, Selivonin I V and Moralev I A 2017 *Phys. Plasmas* **24** 103528
[111] Okumura T, Zhou C, Kubo E, Shimizu T, Nakajima T and Sato T 2018 *Appl. Phys. Express* **11** 016201
[112] Kawasaki T, Terashima T, Takada T and Maeno T 1994 *J. Phys. D: Appl. Phys.* **27** 010
[113] Iseni S 2020 *Plasma Res. Express* **2** 025014
[114] Brahme A, Chang Z, Zhao N, Kondeti V S S K and Bruggeman P J 2018 *J. Phys. D: Appl. Phys.* **51** 414002
[115] Takada T 1999 *IEEE Trans. Dielectr. Electr. Insul.* **6** 519–47
[116] Abolmasov S N, Abo R, Shirafuji T and Tachibana K 2006 *Jpn. J. Appl. Phys.* **45** 8255–9
[117] Tanaka D, Matsuoka S, Kumada A and Hidaka K 2009 *J. Phys. D: Appl. Phys.* **42** 075204
[118] Slikboer E, Guaitella O and Sobota A 2016 *Plasma Sources Sci. Technol.* **25** 03LT04
[119] Sugimoto K, Takahashi H, Shimomura O and Sakurai T 2003 *J. Phys. D: Appl. Phys.* **36** 2887–90
[120] Sam Y, Swingler S, Sutton S, Wilkinson J, Lewin P and Davies A 2003 *IEE Proc.* **150** 43–52
[121] Tschiersch R, Nemschokmichal S, Bogaczyk M and Meichsner J 2017 *J. Phys. D: Appl. Phys.* **50** 105207
[122] Jeong D C, Bae H S and Whang K W 2005 *J. Appl. Phys.* **97** 013304
[123] Gégot F, Callegari T, Aillerie M and Boeuf J P 2008 *J. Phys. D: Appl. Phys.* **41** 135204
[124] Wu A S *et al* 2013 *J. Surg. Res.* **179** e1–e12
[125] Pechereau F, Jánský J and Bourdon A 2012 *Plasma Sources Sci. Technol.* **21** 055011
[126] Mu H and Zhang G 2011 *Plasma Sci. Technol.* **13** 645–50
[127] Li T, Yan H-J, Li J-Q, Schulze J, Yu S-Q, Song J and Zhang Q-Z 2022 *Plasma Sources Sci. Technol.* **31** 055016
[128] Slikboer E, Garcia-Caurel E, Guaitella O and Sobota A 2017 *Plasma Sources Sci. Technol.* **26** 035002
[129] Stollenwerk L, Laven J G and Purwins H-G 2007 *Phys. Rev. Lett.* **98** 255001
[130] Slikboer E, Viegas P, Bonaventura Z, Garcia-Caurel E, Sobota A, Bourdon A and Guaitella O 2019 *Plasma Sources Sci. Technol.* **28** 095016

[131] Bogaczyk M, Wild R, Stollenwerk L and Wagner H-E 2012 *J. Phys. D: Appl. Phys.* **45** 465202
[132] Wild R, Gerling T, Bussiahn R, Weltmann K-D and Stollenwerk L 2014 *J. Phys. D: Appl. Phys.* **47** 042001
[133] Slikboer E 2015 Electric field and charge measurements in plasma bullets using the pockels effect *PhD Thesis* Eindhoven University of Technology
[134] Slikboer E, Guaitella O, Garcia-Caurel E and Sobota A 2022 *Sci. Rep.* **12** 1157
[135] Razavizadeh S, Ghomi H and Sobota A 2018 *Plasma Sources Sci. Technol.* **27** 075016
[136] Guaitella O, Thevenet F, Guillard C and Rousseau A 2006 *J. Phys. D: Appl. Phys.* **39** 2964–72
[137] Guaitella O, Marinov I and Rousseau A 2011 *Appl. Phys. Lett.* **98** 071502
[138] Golubovskii Y B, Maiorov V A, Behnke J and Behnke J F 2002 *J. Phys. D: Appl. Phys.* **35** 751–61
[139] Ambrico P F, Ambrico M, Colaianni A, Schiavulli L, Dilecce G and De Benedictis S 2010 *J. Phys. D: Appl. Phys.* **43** 325201
[140] Tschiersch R, Bogaczyk M and Wagner H-E 2014 *J. Phys. D: Appl. Phys.* **47** 365204
[141] Peeters F J J, Rumphorst R F and van de Sanden M C M 2016 *Plasma Sources Sci. Technol.* **25** 03LT03
[142] Azzam R and Bashara N 1987 *Ellipsometry and Polarized Light* (Elsevier Science Pub. Co.)
[143] Luan P and Oehrlein G S 2018 *J. Phys. D: Appl. Phys.* **51** 135201
[144] Knoll A J, Luan P, Bartis E A J, Hart C, Raitses Y and Oehrlein G S 2014 *Appl. Phys. Lett.* **105** 171601
[145] Bartis E A J, Knoll A J, Luan P, Seog J and Oehrlein G S 2016 *Plasma Chem. Plasma Process.* **36** 121–49
[146] Garcia-Caurel E, Ossikovski R, Foldyna M, Pierangelo A, Drévillon B and De Martino A 2013 Advanced Mueller ellipsometry instrumentation and data analysis *Ellipsometry at the Nanoscale* (Springer) pp 31–143 (available at: http://link.springer.com/10.1007/978-3-642-33956-1_2)
[147] Philpott H, Garcia-Caurel E, Guaitella O and Sobota A 2023 *Opt. Express* **31** 25585
[148] Philpott H, Garcia-Caurel E, Guaitella O and Sobota A 2021 *Appl. Opt.* **60** 9594
[149] Slikboer E, Sobota A, Guaitella O and Garcia-Caurel E 2018 *J. Phys. D: Appl. Phys.* **51** 115203
[150] Slikboer E, Acharya K, Sobota A, Garcia-Caurel E and Guaitella O 2020 *Sci. Rep.* **10** 2712
[151] Slikboer E, Sobota A, Garcia-Caurel E and Guaitella O 2020 *Sci. Rep.* **10** 13580
[152] Schmidt-Bleker A, Reuter S and Weltmann K-D 2015 *J. Phys. D: Appl. Phys.* **48** 175202
[153] Archambault-Caron M, Gagnon H, Nisol B, Piyakis K and Wertheimer M R 2015 *Plasma Sources Sci. Technol.* **24** 045004
[154] Du C, Liu Y, Huang Y, Li Z, Men R, Men Y and Tang J 2016 *Sci. Rep.* **6** 18838
[155] Nozaki T, Hiroyuki T and Okazaki K 2006 *Energy Fuels* **20** 339–45
[156] Van Turnhout J, Aceto D, Travert A, Bazin P, Thibault-Starzyk F, Bogaerts A and Azzolina-Jury F 2022 *Catal. Sci. Technol.* **12** 6676–86
[157] Kim M and Mangolini L 2024 *J. Phys. Chem. Lett.* **15** 4136–41
[158] Massines F and Gouda G 1998 *J. Phys. D: Appl. Phys.* **31** 3411–20
[159] Jung S H, Park S M, Park S H and Kim S D 2004 *Ind. Eng. Chem. Res.* **43** 5483–8
[160] Lommatzsch U, Pasedag D, Baalmann A, Ellinghorst G and Wagner H-E 2007 *Plasma Process. Polym.* **4** S1041–5
[161] Akishev Y, Grushin M, Dyatko N, Kochetov I, Napartovich A, Trushkin N, Minh Duc T and Descours S 2008 *J. Phys. D: Appl. Phys.* **41** 235203
[162] Albaugh J, O'Sullivan C and O'Neill L 2008 *Surf. Coat. Technol.* **203** 844–7
[163] Kostov K, Nishime T, Castro A, Toth A and Hein L 2014 *Appl. Surf. Sci.* **314** 367–75
[164] Nisol B and Reniers F 2015 *J. Electron Spectrosc. Relat. Phenom.* **200** 311–31
[165] Hueso J, Espinós J, Caballero A, Cotrino J and González-Elipe A 2007 *Carbon* **45** 89–96
[166] Gibson E K *et al* 2017 *Angew. Chem., Int. Ed.* **56** 9351–5
[167] Tomko J A, Johnson M J, Boris D R, Petrova T B, Walton S G and Hopkins P E 2022 *Nat. Commun.* **13** 2623
[168] Grünewald L, Chezganov D, De Meyer R, Orekhov A, Van Aert S, Bogaerts A, Bals S and Verbeeck J 2024 *Adv. Mater. Technol.* **9** 1–16
[169] Saito A, Sheng Z and Nozaki T 2021 *Int. J. Plasma Environ. Sci. Technol.* **15** 1–12
[170] Knust S, Ruhm L, Kuhlmann A, Meinderink D, Bürger J, Lindner J K N, de los Arcos de Pedro M T and Grundmeier G 2021 *J. Raman Spectrosc.* **52** 1237–45
[171] Pai D Z, Pailloux F and Babonneau D 2019 *Plasma Sources Sci. Technol.* **28** 085007
[172] Christensen P A, Ali A H B M, Mashhadani Z T A W, Carroll M A and Martin P A 2018 *Plasma Chem. Plasma Process.* **38** 461–84
[173] Christensen P A, Ali A H B M, Mashhadani Z T A W and Martin P A 2018 *Plasma Chem. Plasma Process.* **38** 293–310
[174] Nitschke M and Meichsner J 1997 *J. Appl. Polym. Sci.* **65** 381–90
[175] Rai V R, Vandalon V and Agarwal S 2010 *Langmuir* **26** 13732–5
[176] Klages C, Hinze A and Khosravi Z 2013 *Plasma Process. Polym.* **10** 948–58
[177] Schäfer J, Fricke K, Mika F, Pokorná Z, Zajíčková L and Foest R 2017 *Thin Solid Films* **630** 71–78
[178] Zhang S and Oehrlein G S 2021 *J. Phys. D: Appl. Phys.* **54** 213001
[179] Stere C E, Adress W, Burch R, Chansai S, Goguet A, Graham W G and Hardacre C 2015 *ACS Catal.* **5** 956–64
[180] Knoll A J, Zhang S, Lai M, Luan P and Oehrlein G S 2019 *J. Phys. D: Appl. Phys.* **52** 225201
[181] Zhang S, Li Y, Knoll A and Oehrlein G S 2020 *J. Phys. D: Appl. Phys.* **53** 215201
[182] Hinshelwood M and Oehrlein G S 2023 *Plasma Sources Sci. Technol.* **32** 125001
[183] Rodrigues A, Tatibouët J-M and Fourré E 2016 *Plasma Chem. Plasma Process.* **36** 901–15
[184] Xu S *et al* 2019 *Nat. Catal.* **2** 142–8
[185] Sheng Z, Kim H-H, Yao S and Nozaki T 2020 *Phys. Chem. Chem. Phys.* **22** 19349–58
[186] Stere C, Chansai S, Gholami R, Wangkawong K, Singhania A, Goguet A, Inceesungvorn B and Hardacre C 2020 *Catal. Sci. Technol.* **10** 1458–66
[187] Parastaev A, Kosinov N and Hensen E J M 2021 *J. Phys. D: Appl. Phys.* **54** 264004
[188] Rivallan M, Fourré E, Aiello S, Tatibouët J and Thibault-Starzyk F 2012 *Plasma Process. Polym.* **9** 850–4
[189] Aceto D, Bacariza M C, Travert A, Henriques C and Azzolina-Jury F 2023 *Catalysts* **13** 481
[190] Wu J, Xia Q, Wang H and Li Z 2014 *Appl. Catal.* B **156-157** 265–72
[191] Jia Z and Rousseau A 2016 *Sci. Rep.* **6** 31888
[192] Clarke R J and Hicks J C 2022 *ACS Eng. Au* **2** 535–46
[193] Winter L R, Ashford B, Hong J, Murphy A B and Chen J G 2020 *ACS Catal.* **10** 14763–74

[194] Garcia-Soto C A, Baratte E, Silva T, Guerra V, Parvulescu V I and Guaitella O 2023 *Plasma Chem. Plasma Process.* **44** 1287–326
[195] Jia Z, Wang X, Thevenet F and Rousseau A 2017 *Plasma Process. Polym.* **14** 1–10
[196] Azzolina-Jury F and Thibault-Starzyk F 2017 *Top. Catal.* **60** 1709–21
[197] Lee G, Go D B and O'Brien C P 2021 *ACS Appl. Mater. Interfaces* **13** 56242–53
[198] Bonn M, Ueba H and Wolf M 2005 *J. Phys.: Condens. Matter* **17** S201–20
[199] Zhang Z, Piatkowski L, Bakker H J and Bonn M 2011 *Nat. Chem.* **3** 888–93
[200] Vandalon V and Kessels W M M E 2017 *J. Vac. Sci. Technol.* A **35** 05C313
[201] Kim H-H, Ogata A, Schiorlin M, Marotta E and Paradisi C 2011 *Catal. Lett.* **141** 277–82
[202] Parastaev A, Hoeben W F L M, van Heesch B E J M, Kosinov N and Hensen E J M 2018 *Appl. Catal.* B **239** 168–77
[203] Mizushima T, Matsumoto K, Ohkita H and Kakuta N 2007 *Plasma Chem. Plasma Process.* **27** 1–11
[204] Navascués P, Obrero-Pérez J M, Cotrino J, González-Elipe A R and Gómez-Ramírez A 2020 *ACS Sustain. Chem. Eng.* **8** 14855–66
[205] Klarenaar B L M, Guaitella O, Engeln R and Sobota A 2018 *Plasma Sources Sci. Technol.* **27** 085004
[206] Simoncelli E, Stancampiano A, Boselli M, Gherardi M and Colombo V 2019 *Plasma* **2** 369–79
[207] Wang R, Xu H, Zhao Y, Zhu W, Ostrikov K K and Shao T 2019 *J. Phys. D: Appl. Phys.* **52** 074002
[208] Adress W and Graham B 2021 *Plasma Sources Sci. Technol.* **30** 095015
[209] Xu G, Geng Y, Li X, Shi X and Zhang G 2021 *Plasma Sci. Technol.* **23** 095401
[210] Liu Z, Wang W, Pang B, Wang S, Gao Y, Xu D and Liu D 2021 *J. Phys. D: Appl. Phys.* **54** 395202
[211] Viegas P, Slikboer E, Bonaventura Z, Guaitella O, Sobota A and Bourdon A 2022 *Plasma Sources Sci. Technol.* **31** 053001
[212] Viegas P *et al* 2020 *Plasma Sources Sci. Technol.* **29** 095011
[213] Cosimi J, Merbahi N, Marchal F, Eichwald O and Yousfi M 2022 *J. Phys. D: Appl. Phys.* **55** 145201
[214] van Rooij O, Wubs J, Höft H and Sobota A 2024 *J. Phys. D: Appl. Phys.* **57** 115201
[215] Cosimi J, Marchal F, Merbahi N, Eichwald O, Gardou J P and Yousfi M 2023 *Plasma Sources Sci. Technol.* **32** 065012
[216] Martinez L, Dhruv A, Lin L, Balaras E and Keidar M 2019 *Plasma Sources Sci. Technol.* **28** 115002
[217] Trelles J P 2016 *J. Phys. D: Appl. Phys.* **49** 393002
[218] Wu K, Zhao N, Wu J, Zhang F, Niu M, Ran J, Jia P and Li X 2022 *Plasma Process. Polym.* **19** 1–9
[219] Bruggeman P and Brandenburg R 2013 *J. Phys. D: Appl. Phys.* **46** 464001
[220] Brandenburg R 2017 *Plasma Sources Sci. Technol.* **26** 053001
[221] Zaplotnik R, Primc G and Vesel A 2021 *Appl. Sci.* **11** 2275
[222] Reuter S, Sousa J S, Stancu G D and Hubertus van Helden J-P 2015 *Plasma Sources Sci. Technol.* **24** 054001
[223] Ono R 2016 *J. Phys. D: Appl. Phys.* **49** 083001
[224] Gazeli K, Lombardi G, Aubert X, Duluard C Y, Prasanna S and Hassouni K 2021 *Plasma* **4** 145–71
[225] Große-Kreul S, Hübner S, Schneider S, Ellerweg D, von Keudell A, Matejčík S and Benedikt J 2015 *Plasma Sources Sci. Technol.* **24** 044008
[226] Benedikt J, Kersten H and Piel A 2021 *Plasma Sources Sci. Technol.* **30** 033001
[227] Niemi K, Reuter S, Graham L M, Waskoenig J and Gans T 2009 *Appl. Phys. Lett.* **95** 1–4
[228] Steuer D, van Impel H, Gibson A R, Schulz-von der Gathen V, Böke M and Golda J 2022 *Plasma Sources Sci. Technol.* **31** 10LT01
[229] Winzer T, Steuer D, Schüttler S, Blosczyk N, Benedikt J and Golda J 2022 *J. Appl. Phys.* **132** 183301
[230] Yang Q, Qiao J-J, Sun F-L, Wang L-C and Xiong Q 2024 *J. Phys. D: Appl. Phys.* **57** 31LT01
[231] Van Doremaele E R W, Kondeti V S S K and Bruggeman P J 2018 *Plasma Sources Sci. Technol.* **27** 095006
[232] Schäfer J, Foest R, Reuter S, Kewitz T, Šperka J and Weltmann K-D 2012 *Rev. Sci. Instrum.* **83** 103506
[233] Kelly S, Golda J, Turner M M and Schulz-von der Gathen V 2015 *J. Phys. D: Appl. Phys.* **48** 444002
[234] Traldi E, Boselli M, Simoncelli E, Stancampiano A, Gherardi M, Colombo V and Settles G S 2018 *EPJ Tech. Instrum.* **5** 23
[235] Xiong Q, Nikiforov A Y, González M A, Leys C and Lu X P 2012 *Plasma Sources Sci. Technol.* **22** 015011
[236] Nikiforov A Y, Leys C, Gonzalez M A and Walsh J L 2015 *Plasma Sources Sci. Technol.* **24** 034001
[237] Bruggeman P, Ribežl E, Maslani A, Degroote J, Malesevic A, Rego R, Vierendeels J and Leys C 2008 *Plasma Sources Sci. Technol.* **17** 025012
[238] Cvetanović N, Galmiz O, Synek P, Zemánek M, Brablec A and Hoder T 2018 *Plasma Sources Sci. Technol.* **27** 025002
[239] Bolouki N, Hsieh J-H, Li C and Yang Y-Z 2019 *Plasma* **2** 283–93
[240] Yang Q, Qiao J, Cheng H, Wang D, Zhang Q, Wang X and Xiong Q 2023 *Plasma Process. Polym.* **20** 1–17
[241] Behmani D and Bhattacharjee S 2023 *Phys. Plasmas* **30** 113503
[242] Rooij O V, Ahlborn O and Sobota A 2024 *J. Phys. D: Appl. Phys.* **57** 385206
[243] Simeni M S, Roettgen A, Petrishchev V, Frederickson K and Adamovich I V 2016 *Plasma Sources Sci. Technol.* **25** 064005
[244] Yue Y and Bruggeman P J 2022 *Plasma Sources Sci. Technol.* **31** 124004
[245] Bourdon A, Darny T, Pechereau F, Pouvesle J-M, Viegas P, Iséni S and Robert E 2016 *Plasma Sources Sci. Technol.* **25** 035002
[246] Goldberg B M, Hoder T and Brandenburg R 2022 *Plasma Sources Sci. Technol.* **31** 073001
[247] Kozlov K V, Wagner H-E, Brandenburg R and Michel P 2001 *J. Phys. D: Appl. Phys.* **34** 3164–76
[248] Paris P, Aints M, Valk F, Plank T, Haljaste A, Kozlov K V and Wagner H-E 2006 *J. Phys. D: Appl. Phys.* **39** 2636–9
[249] Starikovskaia S M, Allegraud K, Guaitella O and Rousseau A 2010 *J. Phys. D: Appl. Phys.* **43** 124007
[250] Stepanyan S A, Soloviev V R and Starikovskaia S M 2014 *J. Phys. D: Appl. Phys.* **47** 485201
[251] Bonaventura Z, Bourdon A, Celestin S and Pasko V P 2011 *Plasma Sources Sci. Technol.* **20** 035012
[252] Obrusník A, Bílek P, Hoder T, Šimek M and Bonaventura Z 2018 *Plasma Sources Sci. Technol.* **27** 085013
[253] Kuraica M M and Konjević N 1997 *Appl. Phys. Lett.* **70** 1521–3
[254] Sretenović G B, Krstić I B, Kovačević V V, Obradović B M and Kuraica M M 2014 *J. Phys. D: Appl. Phys.* **47** 102001
[255] Hofmans M and Sobota A 2019 *J. Appl. Phys.* **125** 043303
[256] Sobota A, Guaitella O, Sretenović G B, Kovačević V V, Slikboer E, Krstić I B, Obradović B M and Kuraica M M 2019 *Plasma Sources Sci. Technol.* **28** 045003
[257] Lempert W R and Adamovich I V 2014 *J. Phys. D: Appl. Phys.* **47** 433001
[258] Ito T, Kobayashi K, Czarnetzki U and Hamaguchi S 2010 *J. Phys. D: Appl. Phys.* **43** 062001

[259] Goldberg B M, Shkurenkov I, Adamovich I V and Lempert W R 2016 *Plasma Sources Sci. Technol.* **25** 45008
[260] Ito T, Kobayashi K, Mueller S, Luggenhölscher D, Czarnetzki U and Hamaguchi S 2009 *J. Phys. D: Appl. Phys.* **42** 092003
[261] Simeni Simeni M, Goldberg B M, Zhang C, Frederickson K, Lempert W R and Adamovich I V 2017 *J. Phys. D: Appl. Phys.* **50** 184002
[262] Simeni M S, Baratte E, Zhang C, Frederickson K and Adamovich I V 2018 *Plasma Sources Sci. Technol.* **27** 015011
[263] Dogariu A, Goldberg B M, O'Byrne S and Miles R B 2017 *Phys. Rev. Appl.* **7** 024024
[264] Chng T L, Starikovskaia S M and Schanne-Klein M-C 2020 *Plasma Sources Sci. Technol.* **29** 125002
[265] Chng T L, Pai D Z, Guaitella O, Starikovskaia S M and Bourdon A 2022 *Plasma Sources Sci. Technol.* **31** 015010
[266] Adamovich I V, Butterworth T, Orriere T, Pai D Z, Lacoste D A and Cha M S 2020 *J. Phys. D: Appl. Phys.* **53** 145201
[267] Mrkvičková M, Kuthanová L, Bílek P, Obrusník A, Navrátil Z, Dvořák P, Adamovich I, Šimek M and Hoder T 2023 *Plasma Sources Sci. Technol.* **32** 065009
[268] Raskar S, Adamovich I V, Konina K and Kushner M J 2024 *Plasma Sources Sci. Technol.* **33** 025010
[269] Bruggeman P J, Sadeghi N, Schram D C and Linss V 2014 *Plasma Sources Sci. Technol.* **23** 023001
[270] Bruggeman P, Schram D C, Kong M G and Leys C 2009 *Plasma Process. Polym.* **6** 751–62
[271] Muñoz J, Dimitrijević M, Yubero C and Calzada M 2009 *Spectrochim. Acta* B **64** 167–72
[272] Weltmann K-D, Kindel E, Brandenburg R, Meyer C, Bussiahn R, Wilke C and von Woedtke T 2009 *Contrib. Plasma Phys.* **49** 631–40
[273] Wertheimer M R, Ahlawat M, Saoudi B and Kashyap R 2012 *Appl. Phys. Lett.* **100** 201112